The International Journal of Advanced Manufacturing Technology (2018) 97:1071–1098
https://doi.org/10.1007/s00170-018-2030-x

ORIGINAL ARTICLE

A review on laser beam welding of titanium alloys

S. T. Auwal[1,2] · S. Ramesh[1] · F. Yusof[1] · S. M. Manladan[3]

Received: 14 February 2018 / Accepted: 10 April 2018 / Published online: 20 April 2018

Abstract
In recent years, there is an increased in used of titanium alloys for some parts of mass-produced automobiles and aerospace. However, titanium alloys are characterized by difficult machinability, high melting temperature, high strength, low thermal conductivity, and high reactivity to oxygen, which overshadowed conventional manufacturing processes. To this end, there is a pressing need for more efficient technologies for the manufacture of low-cost titanium structures. Over the years, several joining techniques have been considered for fabrication of titanium alloys. Nevertheless, laser beam welding presents a viable option for welding of titanium due its versatility, high specific heat input, and flexibility. To date, under optimum processing conditions, the strength of the laser-welded titanium alloys can be close to the original material; however, there are still some processing problems such as lower elongation and corrosion resistance coupled with inferior fatigue properties. In this document, the laser beam welding of similar and dissimilar titanium alloys is reviewed, focusing on the influence of the processing parameters, microstructure-property relationship, metallurgical defects, and possible remedies.

Keywords Review · Laser welding · Titanium alloys · Microstructure · Defect · Mechanical property, dissimilar welding

1 Introduction

With growing concern on the energy and environmental challenges by the day, considerable efforts have been rededicated toward minimizing the fuel consumption and exhaust gas emission in automotive industries around the globe. Several authors suggested that the weight reduction of energy consuming components with light structural materials such as aluminum, magnesium, and titanium is considered as a promising approach to achieve this goal [1–5].

✉ S. Ramesh
ramesh79@um.edu.my

[1] Center for Advanced Manufacturing and Materials Processing (AMMP), Department of Mechanical Engineering, Faculty of Engineering, University of Malaya, 50603 Kuala Lumpur, Malaysia

[2] Department of Mechanical Engineering, Faculty of Engineering, Kano University of Science and Technology, Wudil, Kano 3244, Nigeria

[3] Department of Mechanical Engineering, Faculty of Engineering, Bayero University, Kano, Kano 3011, Nigeria

Titanium and its alloys are one of the commonly used engineering materials in many areas of applications ranging from aerospace, medical, biomedical, biomaterial, petrochemical industries because of their low density, excellent corrosion resistance, high strength, and biocompatibility [3, 6–12]. Titanium alloys are characterized by difficult machinability, high melting temperature, high strength, low thermal conductivity, and high reactivity to oxygen at typical welding temperatures. These inherent material properties impose stringent demands to the welding conditions. With recent advancements in welding technologies, a number of joining techniques have been developed for joining of titanium alloys with the main objective of improving the weld quality, high efficiency, cost-effectiveness, and safety. However, among the welding techniques, laser welding recently gained popularity as a promising joining technology for titanium alloys in industries because of its high precision, high weld quality, high efficiency, excellent flexibility, in addition to low deformation and distortion compared to other traditional welding processes [13–20].

Nevertheless, the laser welding techniques for titanium alloy is a complicated process due to uneven temperature, nonuniform chemical composition, and stress. Furthermore, change in the heat input affects the weld microstructure and

mechanical properties due to poor thermal conductivity of titanium alloys [21]. Moreover, the capital cost of laser welding is significantly higher than the traditional fusion processes although it can be compensated with high and excellent joint quality. Additionally, accurate beam and joint alignment, safety requirements and the severe clamping and fitting, and surface preparation before the welding are necessary for obtaining a good quality weld [11, 22–30]. To better understand and address these challenges, there is a need to comprehensively review the research conducted so far and provide the most efficient strategies to address the challenges. Based on the existing literatures, a great deal of research has been conducted on the mechanical properties and microstructure of the laser beam welded titanium alloys joints, particularly under static loading condition [11, 21, 31, 32]. Under optimized processing conditions, the static strength of the laser-welded titanium alloy samples can be close to the original material; however, there are still some processing problems such as lower elongation and corrosion resistance coupled with inferior fatigue properties [11, 33, 34].

At present, titanium alloys are joined to other metals by laser beam welding under optimized processing conditions. Particularly, Ti/steel, Ti/Al, and Ti/Mg dissimilar alloys have been studies for their mechanical and metallurgical properties. Due to the variation in the work hardening exponents of dissimilar alloys, the formation of intermetallic compounds (IMCs) at the interfaces is expected during cooling stages. A variety of processing conditions with respect to the formations and effects of the IMCs in relation to structure-property relationships has been studied and correlated in literature [35–37]. Therefore, the potentials of laser welding techniques for joining titanium to metals are also reviewed, with focus on the strategies used to control the morphology and existence state of intermediate phase and improving the mechanical properties.

The general motives behind this review are to critically examine the current state of the art and the future trends in laser beam welding of titanium alloys and serve as foundation for reliable laser welding production of titanium alloy joints.

2 Laser welding techniques for titanium alloys

2.1 Laser welding mode

Generally, depending on the heat input, conduction and keyhole mode laser welding have been reported [19]. The conduction mode has a laser power density of less than 10^3 W/cm^2, and the energy absorbed is transferred to the entire weld metal by conduction only (Fig. 1a). Conduction mode has an aspect ratio of less than 0.5, low coupling efficiency, and low welding depth [10, 38, 39]. In contrast, the keyhole mode is generally characterized as a high-energy process in the range of 10^5–10^7 W/cm^2. Keyhole is formed inside the weld zone due to the high power density which causes vaporization of the metal as shown in Fig. 1b. Under keyhole mode, the aspect ratio is above 0.7, narrower fusion zone and heat-affected zone, and high efficiency and high welding depth were reported [19, 34, 39–42]. For titanium alloys weld, keyhole mode is mostly used because of the high input energy required [19, 39].

2.2 Laser welding processing parameters

The main challenge in laser welding of titanium alloys is the selection of the optimum process parameters for achieving better weld quality. Some of the most significant laser welding processing parameters and their impacts on the welding process under keyhole mode are deliberated in this section.

2.2.1 Laser heat source

Titanium alloys are joined by different laser heat sources such as Nd:YAG [13, 23, 34, 39, 43, 44], CO_2 [7, 14, 22, 45], diode [38, 46], disk [27, 32, 47], and recently developed fiber laser [10, 11, 42, 48–52]. However, CO_2 and Nd:YAG lasers are mostly used. Moreover, Nd:YAG continues to dominate the CO_2 laser as a result of the improvement in the output power, high beam quality, and fiber glass delivery [53]. Therefore, compared with CO_2 laser, Nd:YAG laser is most suitable for titanium alloys because the weldability and efficiency of the titanium alloys weld were found to be higher with Nd:YAG laser [13, 23, 34, 39, 54]. Disk laser source was reported to have high efficiency and beam quality compared to traditional CO_2 and Nd:YAG lasers [55, 56]. On the other hand, diode laser was reported to have a better weld quality compared with disk laser for titanium alloys [46]. For instance, Lisiecki et al. [46] studied the weldability of Ti6Al4V alloy using diode and disk lasers and reported that the diode laser yields a better joint quality. Recently, fiber laser heat source was gaining attention as a suitable welding process for joining titanium and its alloys due of its compact size, high efficiency, and beam quality [11, 51, 52].

2.2.2 Laser power and welding speed

The effect of the welding speed and laser power on the weld shape has also been reported in the literature. Laser power and welding speed affect the weld geometry and quality. Many authors reported that the laser power directly the weld penetration depth while welding speed has an inverse effect [11,

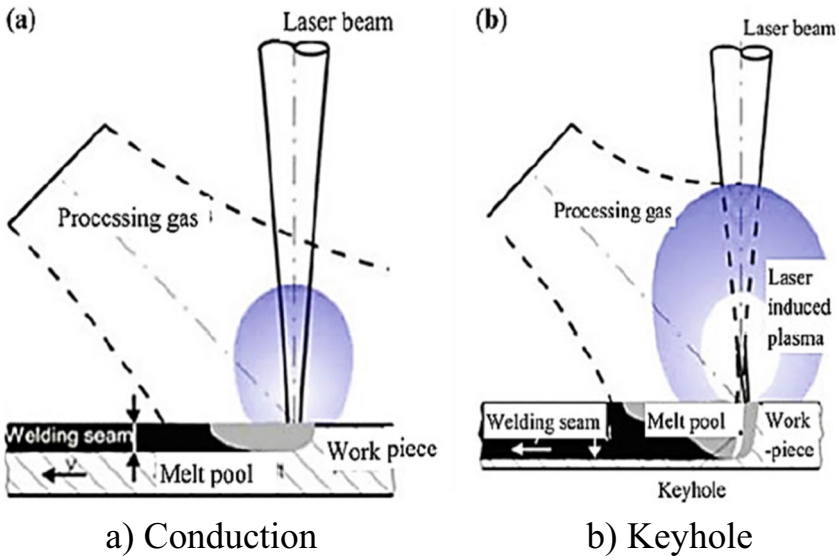

Fig. 1 Laser welding modes [19]

23, 34, 39, 52, 54, 57–63]. For example, Fig. 2 shows the effect of welding speed and laser power on the depth of penetration for Ti6Al4V alloy laser weld. Akman et al. [23] investigated the influence of the laser output parameters on the weld quality for Ti-6Al-4V alloy using pulse Nd:YAG laser. The results indicated that the penetration depth and geometry could be controlled by regulating the laser output parameters (pulse energy and pulse duration). Campanelli et al. [52] laser-welded Ti6Al4V alloy using fiber laser and observed that at constant laser power (1.2 kW) the change of welding speed from 2 to 2.5 m/min transformed the weld bead geometry from nail head to V shape. Mueller et al. [54] found that the weld bead geometry of Ti6Al4V is determined by the welding speed. The authors suggested that the tendency to entrap gases is more likely while welding with high speed. Some authors observed that for fiber laser-welded Ti6Al4V, high welding power led to spatter and undercut, whereas, incomplete penetration occurred at low laser power and high welding speed [60]. On the other hand, Sun et al. [59] compare the bead geometry and microstructure of Ti6Al4V alloy using TIG, plasma, and CO_2 laser heat sources. It was found that the weld geometry depends on the welding speed. Interestingly, the grain size of the laser weldments was observed to be smaller.

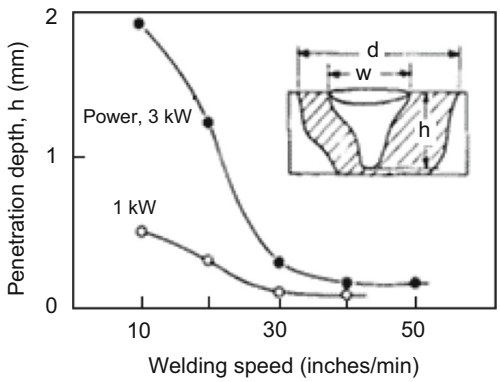

Fig. 2 Effect of welding speed and laser power on the depth of penetration for Ti6Al4V alloy laser weld [57]

2.2.3 Defocused position

Considerable number of studies suggested that the power density is determined by the laser power and the distance between the base metals and the focus plane [11, 23, 55, 60, 64]. Kabir et al. [64] studied the effect of defocusing distance and welding speed on the transverse weld geometry. It was found that both parameters could be optimized to obtain a good quality weld with low geometry defects. Kumar et al. [11] laser welded Ti6Al4V. The defocused position was reported to influence weld geometry. However, the overall fusion zone area remained unaffected. Recently, Caiazzo et al. [55] laser-welded Ti6Al4V sheets in butt configuration using disk laser and reported that the defocusing affect the crown and the root width of the weld.

2.2.4 Operational mode

Both pulsed wave (PW) [13, 23, 43, 65–70] and continuous wave (CW) lasers [22, 34, 45, 71–73] were used for welding of titanium alloys. However, CW is mostly employed because of its higher penetration, excellent beam quality, higher welding efficiency, and, therefore, gained a great attention at present for welding of titanium alloys and will assume a dominant role in the future because of its lower operating and investment costs compared to pulse wave lasers [22, 73]. In comparison, pulsed Nd:YAG laser provides benefit such as lower heat input, less deformation, shorter solidification time, and narrower weld bead and heat-affected zone and, therefore, a PW mode laser is more suitable for welding thin sheet [13, 67, 69, 74].

2.3 Shielding gas

Titanium alloys were reported to be extremely active at high temperatures, particularly in a molten state and readily pick up atmospheric gases, dirt, grease, and refractories leading to embrittlement of the weld pool. Therefore, titanium alloys during laser welding have to be completely shielded in an inert or vacuum environment [6, 7, 22, 23, 75]. Additionally, the use of inert gas during laser welding efficiently protects plume formation and improve the keyhole stability [43, 76, 77]. The widely used inert gas for shielding the titanium alloy welds is argon [10, 30, 78, 79], helium [23, 41, 45], or argon-helium mixtures [22, 34, 39, 80]. However, argon is the most preferred choice for titanium alloys welds [10, 81]. For instance, the influence of shielding gases on the T3-2024 weld quality revealed that both the argon and the helium gases could effectively shield the welds from oxidation. However, under the lowest speed and at the maximum focal position, higher ionization potential and thermal conductivity of helium resulted in an excessive weld width [81].

2.4 Filler materials

The addition of filler wire was reported to eliminate face/root undercut (underfill) and enhance the mechanical properties of the joint. However, the use of filler wire may give more opportunities for hydrogen contamination (porosity) [82–87]. Cao et al. [82] reported that the use of filler wire significantly decreased the underfill defects of Ti-6Al-4V alloy and a relatively high ductility was obtained but slightly increased the porosity for laser welds. Kashaev et al. [85] studied Nd:YAG single-sided laser beam welding of Ti-6Al-4V T-joints using a compatible filler (Titanium Grade 2). The use of filler suppressed the formation of underfills and undercuts. Furthermore, several studies suggested that the use of filler wire helps in modifying the weld zone and make up the loss of volatile alloying elements [84, 88–90]. Cai et al. [91] successfully welded ɣ-TiAl alloy using pure Ti filler metal by laser. The use of filler improved the joint performance and strength by about 74.8%, and an elongation of 94% of the base metal was achieved at room temperature.

2.5 Surface preparation

Titanium alloys are readily oxidized when exposed to atmospheric air and an oxide film is formed on its surface. The oxide layer was reported to largely depend on the composition, structure, morphology, mechanical condition, and temperature. Poor surface preparation and cleaning of the base metals and the filler materials before and during welding and/or poor shielding was reported to be the main factors responsible for the surface oxidation [6, 7, 75, 92]. Therefore, to obtain a sound weld with titanium alloys, the oxide layer and other contaminants need to be thoroughly removed by surface pretreatment. Surface preparation of the titanium alloys was also reported to improve its laser beam absorption [22]. A number of surface preparation treatments were reported, such as sandblasting [57, 75, 82, 93]. Bertrand et al. [93] reported an improved laser beam absorption due to reduced beam reflectivity in commercially pure titanium samples when sandblasted. Recently, the use of more advanced surface treatment based on laser cleaning showed that the surface treatment improved the absorption of laser radiation of titanium alloy surface and the weld penetration [92, 94–97]. Kumar et al. [94] studied the laser cleaning of Ti3Al2.5V alloy. It was found that the laser cleaning treatment improved the laser beam absorption and weld penetration by about 20%, and a defect free weld was produced.

2.6 Joint design

Joint preparation is an important step in laser welding, with appropriate joint preparation, even a very thick section can be laser welded using multipass techniques. The joint design is generally specific in nature depending on the application. Different joint configurations have been applied during laser welding of titanium alloys, such as single-pass V-joint and H-joint [98], T-joint [47, 99, 100], butt [22, 23, 34, 43, 45, 71, 101], and lap [22, 58, 102]. However, butt joints are the most commonly used joint configuration. The general consideration for the butt joint design is that the alignment between the beam and the joint has to be good to prevent concavity due to air gaps [25]. Additionally, the general fit up tolerance for butt-welded joint was reported to be within 15% of the work piece thickness. Misalignment and out-of-flatness should be less than 25% of the work piece thickness [101]. One drawback with butt welding is the difficulty of the joint fit up, which requires extreme precision along the edges to be welded [25]. However, the use of filler metals lowered the strict joint fit up requirement of the butt joint [84, 87, 88, 101, 103]. Sharif et al. [84] reported a full butt joint penetration of Ti5553 plates up to a joint gap of 0.5 mm with a Ti6Al4V filler wire. The authors suggested that the welded joint with filler displayed a smoother transition and minimized the sensitivity to fatigue failure. Furthermore, for thin Ti sheets, some authors suggested that the use of filler metal or edge preparation is not necessary [13]. Accurate fixturing is expensive and time-consuming, but required for successful laser welding of titanium alloys.

3 Microstructural evolution during laser beam welding of titanium alloys

For Ti alloys welds, three distinct regions, i.e., the base metal (BM), the heat-affected zone (HAZ), and the fusion zone (FZ), depending on the temperature were experienced during the

welding operation [23, 34, 72, 84]. The analysis of the microstructure of a typical α titanium alloy (Ti-5Al-2.5Sn) showed that the BM contained fine equiaxed α-grains as shown in Fig. 3a. The fusion zone consists of very fine α′ martensite because of the low heat input and higher cooling rate in the fusion zone (Fig. 3b) [104]. Similar formation of α′ martensite for α titanium alloys was reported by several authors [105, 106]. In contrast, no clear evidence of martensite has been observed in commercially pure titanium (CP-Ti) laser weld bead by some authors [29, 38] due to relatively low cooling rate in the letter treatments. The HAZ contains a mixture of martensite, primary α phases, β phases, and transformed β phases (Fig. 3c). Liu et al. [79] studied the microstructural evolution of the fusion zone of commercially pure titanium alloy (CP-Ti) using fiber laser. The authors found that at a low cooling rate, granular-like grains were formed in the fusion zone. However, with an increasing cooling rate, the microstructure of the fusion zone changed from granular-like to columnar-like. Liu and co-workers suggested that the microstructural evolution of the fusion zone of the pure titanium alloy depends significantly on the β → α phase transformation associated with the cooling rate. Zhang et al. [107] investigated the microstructure and properties of CO_2 Laser-MIG hybrid welded joints for 4-mm-thick Ti-70 alloy (near α-Ti alloy). They found that coarse columnar crystals and isometric crystals, respectively, formed in the welding seam and HAZ, while the FZ composed of coarse α′ martensite and spiculate α microstructure. Recently, Junaid et al. [104] joined Ti5Al2.5Sn by pulsed Ng:YAG and pulsed tungsten inert gas. It was found that the higher cooling rate associated with laser process led to a complete α′ martensitic transformation in the FZ, whereas, due to a lower cooling rate, α′ and acicular α were formed within an equiaxed β matrix in pulse tungsten inert gas welded joints.

The microstructure of a typical laser-welded α+β titanium alloy has also been described in the literature. Generally, the BM consists of two phases: the β-phase dispersed in a dominating α-matrix, the FZ consisted of α′ martensitic structure, and the HAZ consisted of martensitic α′, acicular α, and primary α [10, 23, 34, 38, 39, 41, 58, 71, 74, 87, 108]. The typical microstructure of the laser-welded Ti6Al4V is shown in Fig. 4 [11]. Figure 4a shows the optical micrograph of the BM, HAZ, and FZ of the weld bead, whereas, Fig. 4b, c shows the microstructure of BM. It consists of two phases, β-phase dispersed in a dominating α-matrix. The β-phase with body-centered structure (BCC) is distributed along the boundaries of α-phase. Figure 4d, e shows the optical and FESEM microstructure of the FZ, respectively. It can be seen that the α′ martensitic structure having acicular morphology was formed. Furthermore, a mixture of martensitic α′, acicular α, and primary α was formed in the HAZ. The observed microstructure is typical for laser-welded Ti6Al4V alloy [11, 23, 33, 34, 45, 55]. Cost et al. [10] reported the same martensitic structure at the fusion zone for Ti6Al4V alloy while using fiber laser and a fine cellular dendritic structure at the HAZ. The microstructure morphology of the fusion zone was reported to be significantly dependent on the heat inputs, i.e., at low heat inputs, the weld bead morphology was needle-like which transformed to plate-like at higher heat inputs. Squillace et al. [39] reported that the high heating above the beta transus and fast cooling rate of laser welding were the main cause of martensitic α′ formation. The authors suggested a cooling rate of 410 °C/s for the base metal

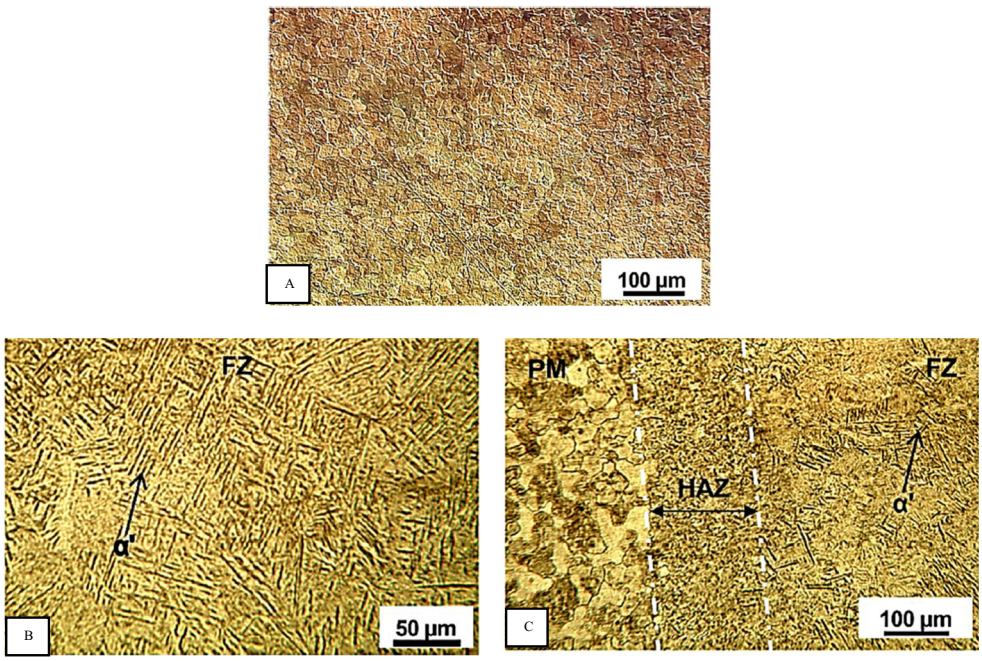

Fig. 3 Microstructure of a typical α-titanium alloy. **a** BM. **b** FZ (α′ martensite formation). **c** FZ/HAZ/BM [104]

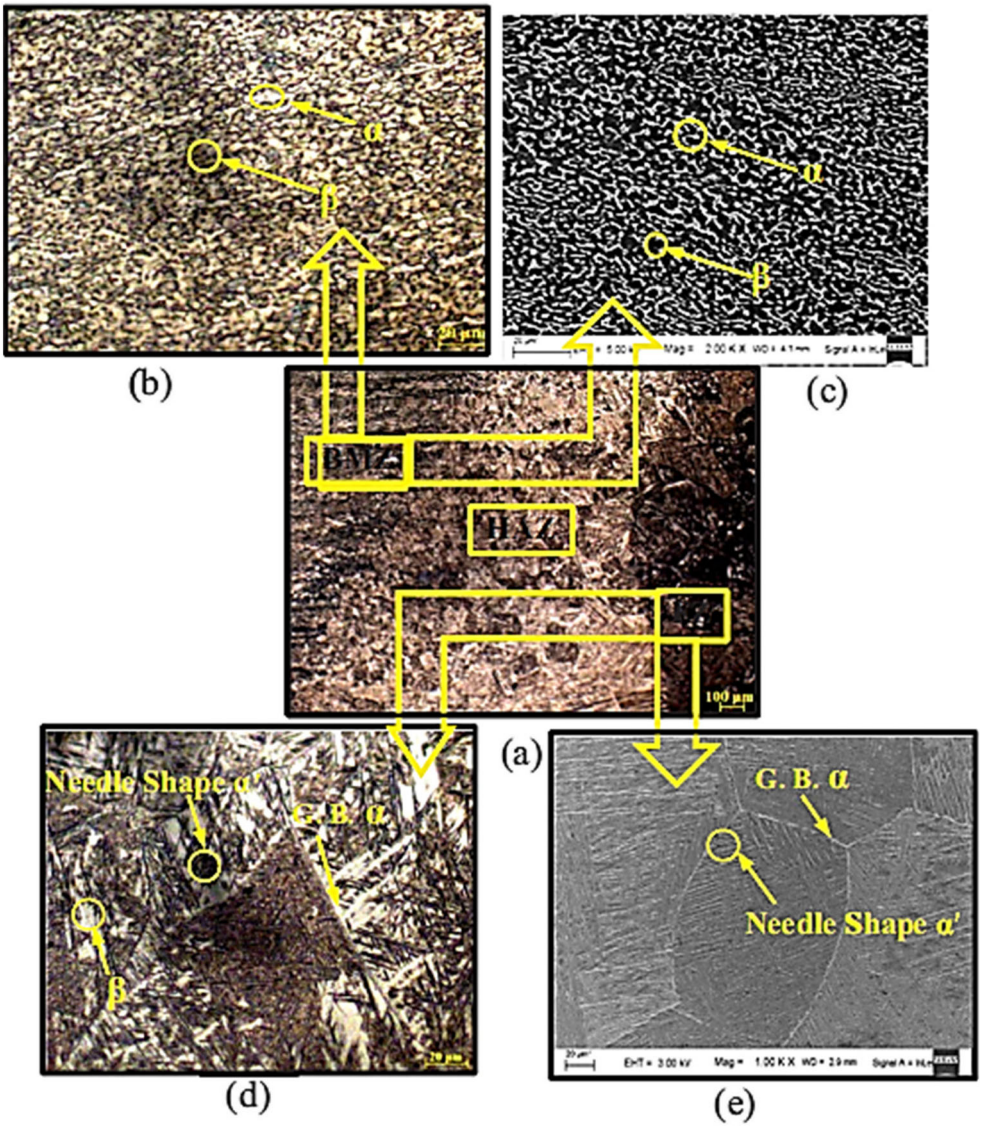

Fig. 4 Typical microstructures of the different zones in the typical α+β alloy laser-welded joint. **a** Optical images consisting BM, HAZ, and FZ. **b** Optical image. **c** FESEM of BM. **d** Optical image. **e** FESEM of FZ [11]

of the Ti6Al4V alloy for a complete transformation to a martensitic α′ phase. Recently, Fomin et al. [33] joined a 2.6-mm-thick Ti6Al4V alloy using CW ytterbium fiber laser. It was found that the fusion zone consists of mainly acicular α′ martensitic structure within the β grains because of the diffusionless β → α' transformation upon high cooling rates.

In recent years, several authors focused on improving the welding properties of titanium aluminide (Ti_2AlNb-based alloys) containing the orthorhombic O phase because of their excellent room and elevated temperatures properties [109] and their microstructure have been systematically investigated. Generally, Ti_2AlNb-based alloys base metal consists of three phases, i.e., α_2, O, and B2 phases, with needle-shaped O phase and spherical α_2 dispersed within the B2 matrix as shown in Fig. 5a [31, 110–113]. Figure 5 shows a typical microstructure of a laser-welded Ti22Al27Nb alloy. It was found that cellular grains whose orientation is perpendicular to the boundary between the fusion zone and the heat-affected zone were generated in the weld (Fig. 5b, c). The FZ of the welded joint was composed of a single B2 phase due to the fast cooling rate in laser beam welding greater than 120 K/s [114] and the high content of niobium [31, 110–113, 115–117]. Boehlert et al. [112] observed that the microstructure of Ti23Al27Nb alloy was fully B2 after 1090 °C solution treatment. Similarly, Wu et al. [113] reported that the microstructure of the Ti-24Al-17Nb laser weld was primarily composed of an ordered B2 phase and independent of laser power.

4 Mechanical properties of titanium alloy laser-welded joints

4.1 Hardness

The hardness of joints is closely related to their microstructure [34, 49, 118]. The inhomogeneity of the microstructure

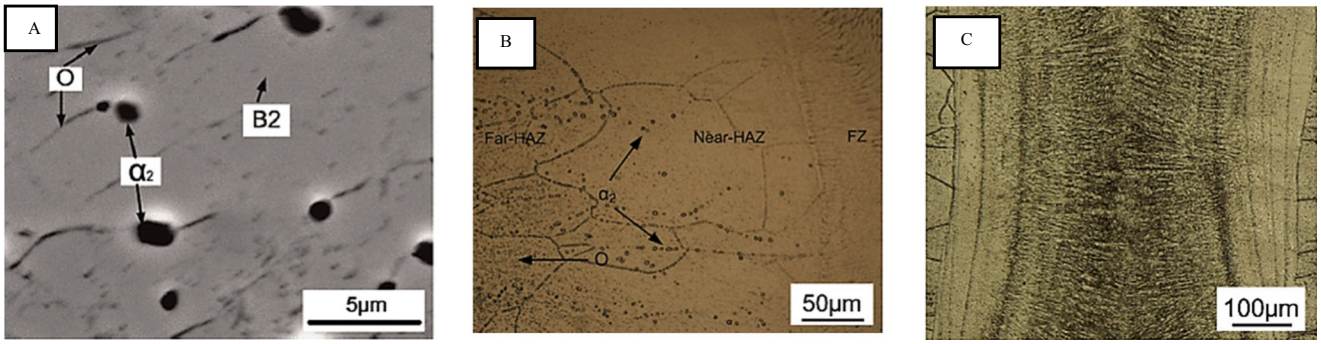

Fig. 5 The microstructure characterization of laser-welded Ti22Al27Nb. **a** BM. **b** HAZ. **c** FZ [31, 52]

resulted in diversity of mechanical properties. Generally, the microhardness and strength of existing phases in the joints follow the order martensite $\alpha' > \alpha$ phase > β phase [118].

For typical α-alloys and near-α alloy, the FZ of the titanium alloy welds was reported to have high microhardness value than the BM, due to the formation of a fine acicular α′ martensitic structure. Then, the microhardness drops rapidly in the adjacent HAZ and the BM has the lowest microhardness value [24, 38, 79, 93, 119]. Amaya et al. [38] observed that for high power diode laser-welded commercially pure titanium alloy (grade 2), the FZ has the highest hardness ranging from 140 to 200 HV compared to the untreated BM (110~140 HV). The highest microhardness obtained in the FZ was associated with formation of acicular α-grains. Wang et al. [119] laser welded 2-mm-thick TA15 alloy and reported that the Vickers' microhardness of the FZ was ranging from 353.86 to 368.81 HV, HAZ has a Vickers' microhardness ranging from 346.00 to 362.91 and the BM Vickers' microhardness ranging from 326.65 to 347.53 HV. Chamanfar et al. [24] found that for laser-welded 76-mm thick Ti6242 alloy, the rapid solidification of the weld pool led to the formation of the acicular α′ martensite with a hexagonal closed packed structure (HCP) in the FZ. The average microhardness of the FZ was 108 HV higher than the BM (328 HV). Recently, Junaid et al. [104] joined Ti-5Al-2.5Sn by pulsed Nd:YAG laser and pulsed tungsten inert gas. The results indicated that the BM has an average microhardness of 343 HV, and the highest microhardness value was found in the FZ of the pulsed laser-welded joint, which is 54.57 HV higher than the microhardness of the BM. Moreover, the average microhardness of the pulsed TIG weldment was found to be 372.38 HV. Generally, the microhardness of the FZ is mainly determine by the martensitic formation, which depends significantly on cooling rates.

Similarly, the highest microhardness was obtained in the FZ for α-β titanium alloys because of the formation of the needle-like martensitic α′ presence in the solidified fusion zone [10, 11, 13, 25, 27, 34, 38, 39, 47, 55, 58, 120–122]. Akman et al. [23] observed the microhardness values ranging between 350 and 500 HV for an α′-martensitic microstructure in 3-mm-thick Ti6Al4V alloy weld, while that of the BM ranges between 300 and 350 HV while using pulsed Nd:YAG laser. Cao et al. [122] reported that for CW Nd:YAG laser-welded 3.2-mm-thick Ti6Al4V alloy, the microhardness increases from the BM (312 ± 8 HV) to the FZ (360 ± 4 HV). Cao et al. [34] laser welded Ti6Al4V alloy with 1- and 2-mm thickness and reported that the FZ has an average microhardness increase of 75 and 58 HV for 1- and 2-mm plates, respectively, compared to BM. The authors observed that the microhardness values of the HAZ and FZ showed no clear tendency to change with welding speed as observed by Sun et al. [59]. Kumar et al. [11] also observed the highest microhardness values at the FZ, ranging from 352 to 368 HV, compared to the base metal zone (BMZ) (305~315 HV) for 5-mm-thick Ti6Al4V alloy using fiber laser heat source. Recently, Fomin et al. [33] joined 2.6-mm-thick Ti6Al4V alloy using CW ytterbium fiber laser. The microhardness distribution is shown in Fig. 6. The BM has an average microhardness of 336 ± 8HV05, whereas, the FZ exhibited the highest average microhardness, approximately 18% greater than for the BM. Fang et al. [73] compared laser-welded Ti-2Al-1.5Mn titanium alloy under pulse wave and continuous wave mode using fiber laser. Figure 7 shows the results of the microhardness distributions across the weld zones. It can be seen that the average microhardness of the FZ was slightly lower

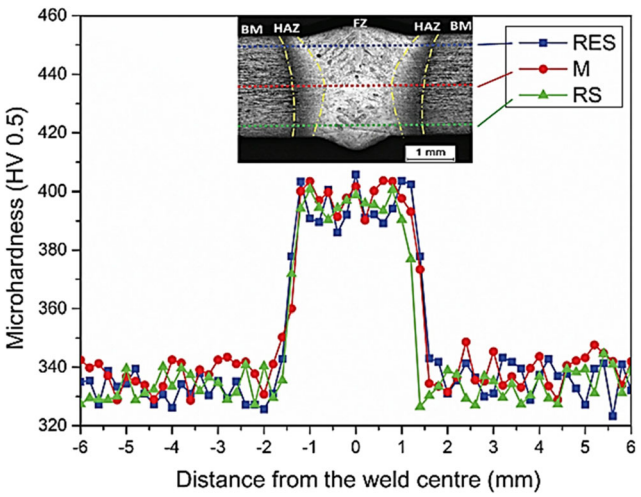

Fig. 6 Vickers' microhardness of laser-welded Ti6Al4V alloy across the weld line [33]

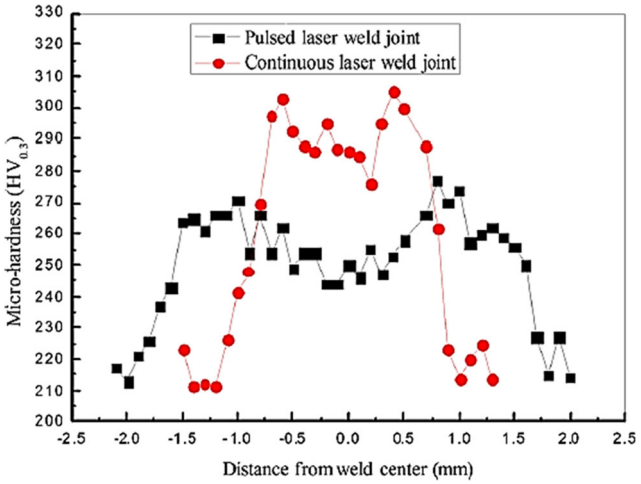

Fig. 7 Microhardness distribution of pulse and continuous wave laser-welded Ti2Al1.5Mn alloy [73]

than that of the fully transformed HAZ: due to the finer α′ martensite structure produced by the faster cooling rate. In contrast with pulse wave joints, the continuous wave welded joints has a higher average microhardness value in the HAZ and FZ due to the decreasing of welding specific heat input. Generally, the significant fluctuations in microhardness values at various zones were mainly associated with differences in grain sizes and phase constituent coupled with closely packed structure of titanium [79].

4.2 Tensile properties

Microstructures play an important role in determining the mechanical properties and fracture behavior of titanium alloys [123]. The tensile strength of the titanium alloy weld was observed to be almost similar to the base metal [34, 41, 48, 61, 70, 76, 78, 119, 122]. Fang et al. [74] observed an average tensile strength of 661 MPa comparable to the BM (642 MPa) for thin Ti2Al1.5Mn butt welds. Similarly, the authors found that the elongation of the FZ (22%) was comparable to that of the BM (24%). Chamanfar et al. [24] reported that for a laser-welded Ti6242, the ultimate tensile strength slightly decreased from 1120 MPa at the BM to 977 ± 4 MPa at the FZ. The yield strength and elongation of the FZ (775 ± 7 MPa, 13.4 ± 0.8%, respectively) were comparable to that of the BM (880 MPa, 19.4%, respectively). However, several authors noted that the presence of weld defects tends to deteriorate the joint mechanical performance. For instance, Cao et al. [34] reported for laser-welded Ti6Al4V alloy, the tensile strength and yield strength slightly increased from the BM (950, 880 MPa, respectively) to FZ (975–1043, 936–987 MPa, respectively). However, a significant decrease in the FZ elongation at fracture (6.5–12.4%) was observed compared to the BM (14%). The obvious decrease in elongation at fracture of the weld was associated to the presence of micropores and aluminum oxide inclusions. Kumar et al. [11] reported that the ultimate tensile strength and elongation of Ti-6Al-4V welds of 872 MPa and 3.74%, respectively, lower than the BM 957 MPa and 11%, respectively. The presence of weld porosity was considered the main cause of the degraded mechanical properties observed.

The strength of the laser-welded Ti_2AlNb-based alloys was reported to be almost similar to that of the base metal [31, 111, 113, 116, 124]. For instance, the tensile strength of Ti-22Al-27Nb was reported to be 1008–1036 MPa at room temperature, close to that of the base metal (1008 MPa). The elongation was found to be 56% of the base metal. However, the tensile strength decreases to about 733 MPa (with an elongation of 2.93%) when tested at 650 °C. The lower ductility of the weld was associated with low O phase slip [31]. Chen et al. [116] also reported high temperature brittle behavior due to nucleation and growth of the O phase during laser welding of Ti-22Al-25Nb alloy. These results suggested that both the strength and the ductility are significantly influenced by temperature.

Moreover, some studies suggested that the joint gap tolerance has a direct effect on the plastic deformation and the percent elongation. However, the joint gap distance has no significant impact on the tensile strength of the titanium alloy welds. Therefore, an appropriate joint gap distance should be maintained for judicious combination of mechanical properties [84, 125, 126]. Sharif et al. [84] recommended that the welding-gap distance to be maintained no less than 0.5 mm for a laser-welded 3.1-mm-thick Ti-5Al-5V-5Mo-3Cr (Ti5553) plate while using CW Nd:YAG laser. Furthermore, several authors suggested that maintaining a high-notched strength is compulsory during tensile straining at elevated temperature. Tsay et al. [40, 127] studied the effect of notched tensile strength on the laser-welded Ti-6Al-6V-2Sn and Ti-4.5Al-3V-2-Fe-2Mo alloys. The notched tensile strength of the welded specimens was found to be much lower than that of the base metal at room temperature. However, reversed tendency was observed at elevated temperature. The joint properties of the as-welded and BM samples decreased with increasing testing temperature and that the post weld heat treatment has helped to maintain the joint properties up to 450 °C.

Based on the existing literatures, the joint strength could be improved by preheating, post heating, or addition of alloying elements [40, 91, 128–130]. Liu et al. [130] studied the influence of in situ and post weld heat treatment on the laser beam spot-welded Ti-42Al-2.5Cr-1Nb-0.7Si-0.5B TiAl-based alloy. It was found that conventional post weld heating for 2 h at 1260 °C significantly improved the mechanical properties. For instance, a maximum ultimate tensile strength of 564 MPa and elongation to fracture of 1.33% at 750 °C was obtained. On the other hand, Cai et al. [91] investigated laser welding TiAl alloy (Ti-48Al-2Nb-2Cr) by using pure Ti filler metal and observed an improvement in the room temperature

tensile strength and elongation of the laser-welded joints to about 288 MPa and 2.19%, respectively, accounting for 74.8 and 94.0% of the BM, respectively.

4.3 Superplasticity

Considerable number of studies suggested that the Ti-6Al-4V is well known to possess an excellent superplastic property under suitable tensile conditions [71, 72, 131]. Joints welded by high-energy beam welding such as electron beam welding and laser beam welding exhibit possibly better superplasticity because of their narrow HAZ and finer grained weld beads. However, the electron beam technique needs a vacuum environment, which limits its industrial application. As consequence, laser-welded titanium sheets may be used for superplastic forming in the production of complex engineering structures [71, 72, 131–134]. Generally, the superplastic behavior of the laser-welded titanium alloys is essentially depends on the welding conditions. Therefore, to achieve an equivalent superplastic performance of the parent metal, optimization of the process parameters is required.

It worth noting that deformed Ti-6Al-4V laser welds also exhibit superplastic behavior [71, 72, 132, 133, 135]. The highest joints elongations reached 397% when deformed in the temperature of 900 °C and 10^{-3}/s strain rate was reported [132]. The stress-strain curves shown in Fig. 8 exhibited softening character of superplastic deformation. When compared with the unwelded samples, the flow stress of the welded specimen was higher and elongation was lower under the same condition. The analysis of the microstructure revealed that the superplastic behavior of Ti-6Al-4V was governed by the α to β phase transformation and grain boundary sliding (GBS) [132, 133]. In turn, dynamic globularization process is enhanced by increasing temperature and decreasing strain rate [132]. In another study, the formability of the laser-welded joints between fine grained and standard Ti-6Al-4V showed that the superplastic forming in the fine grained Ti-6Al-4V sheet was observed without crack formation in the HAZ or the FZ, but the weld seam is resistant to superplastic forming due non-equilibrium thermal process during laser welding [136]. Similarly, Wang et al. [134] studied the mixed dynamic recrystallization mechanism during the globularization process under a hot tensile deformation for laser-welded TA15 alloy at temperature range of 800–900 °C and 1.0×10^{-1} to 1.0×10^{-3}/s strain rate. The authors observed that the continuous globularization is the major hot deformation mechanism for the laser-welded TA15 alloys. However, the dynamic recrystallization plays an important role during the globularization process. A maximum elongation of 292% was achieved at 900 °C, 0.0001 s^{-1}, which exhibits superplastic characteristics.

4.4 Fatigue

Welded joints of titanium alloys are usually subjected to fluctuating loads leading to microcracks, which grow during the life of the joint as fatigue. Therefore, the study of the fatigue crack growth of the titanium alloy welded joints is necessary to prevent the failure with prediction such that the crack will not propagate prior to detection [137]. Generally, evaluating the fatigue life of a welded titanium alloys joints is very difficult because of the interactions between the different factors such as microstructural modifications induced by the thermal cycle, distortions, residual stresses, and local and global geometry of the seam, which affect the fatigue limit of the welded structures by producing stress concentration near the weld toe. Unfortunately, no guidelines are actually available to evaluate the fatigue life for titanium alloys unlike that of steel and aluminum structures [138].

Several researchers reported that the fatigue crack growth resistance of the titanium alloy is significantly reduced by welding process, but titanium alloy laser welds exhibited the highest fatigue growth resistance compared to other traditional fusion processes [14, 15, 28, 39]. For instance, regardless of the heat source, the fatigue resistance of Ti6Al4V alloy was found to be lower than the base metal and laser welding was reported to exhibit the higher fatigue performance. The presence of very fine lamellar shaped α in the weld metal was main reason for the superior fatigue performance observed [14, 15].

For defective welds, fatigue crack is initiated from the weld defects such as porosity and underfill, which degraded the fatigue performance [28, 33, 39, 42]. Tsay et al. [28] reported that for laser-welded Ti6Al4V joints, the effect of fatigue

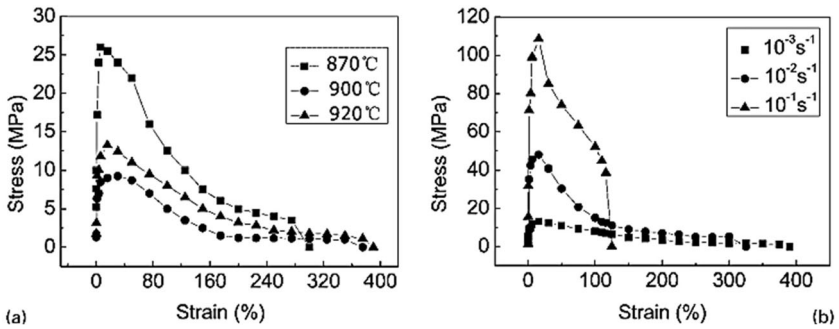

Fig. 8 Typical stress-strain curves of Ti-6Al-4V laser-welded specimens illustrating superplastic behavior [132]

growth resistance was highly significant at higher stress ratio and that the FZ fatigue crack growth resistance was much lower than for the BM. Squillace et al. [39] reported that the underfill radius influences the fatigue performance of laser-welded Ti6Al4V butt joints. Recently, Fomin et al. [33] investigated the high cycle fatigue performance of fiber laser-welded Ti6Al4V butt joints. Underfill and reinforcements in the weld degraded the fatigue performance of the joints. The authors suggested that the fatigue performance of the joints could be improved by machining the weld reinforcements and underfill flush (Fig. 9). The fatigue limit of the BM in the as-received condition was 650 MPa, compared to 720 MPa after milling the surface of the samples, whereas, the fatigue limit after limit after milling the weldment flush increased to 500 MPa. In addition, post weld heating above 750 °C further increased the fatigue limit to 550 MPa.

4.5 Fracture toughness

In laser-welded structures, fracture toughness is believed to be essentially influenced by volume defects and primarily cracks. To evaluate the safety of structure, the investigation of the effect of welding on the fracture toughness is crucial. However, few works have been reported for the fracture toughness of titanium alloys welded joints. Shi et al. [7] studied the effect of laser welding on the fracture toughness of a Ti-6.5Al-2Zr-1Mo-1V sheet. It was found that the fracture toughness of the weld zone in the as-welded condition was lower than for the base metal due to rapid cooling during laser welding, and post weld heat treatment (PWHT) at 650 °C for 2 h further reduced the fracture toughness considerably. The further decrease in the fracture toughness observed after PHWT was associated with the formation of coarsened cast structure in weld metal. Fracture toughness of the weld can be improved by slow cooling or PWHT at or above 760 °C [33].

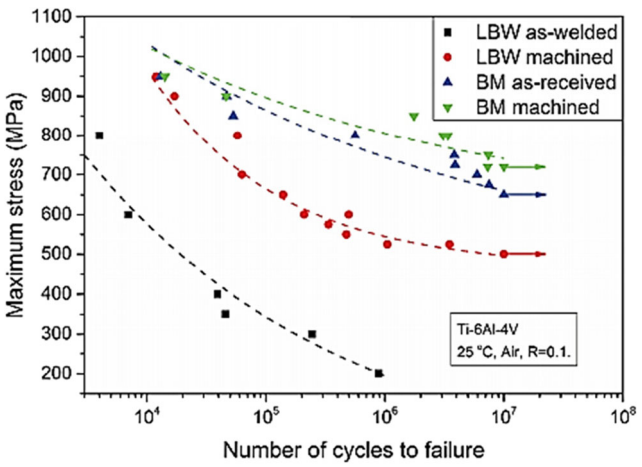

Fig. 9 Fatigue behavior of laser-welded Ti6Al4V alloy [33]

4.6 Corrosion resistance

In view of the potential applications of titanium alloys in medical, chemical, and petrochemical industries, several authors studied the corrosion behavior of the titanium laser welds [38, 105, 139–144]. Compared with many other metals, titanium alloys have excellent corrosion resistance due to the formation of stable, continuous, protective, and adherent oxide film on its surface in the presence of oxygen and moisture, further improvement is still required for some applications such as biomaterials [105]. Generally, the surface characteristics determine the corrosion resistance and, therefore, many surface modification techniques such as laser remelting, laser metal deposition, heat treatment, or cryogenic treatments were adopted to improve the wear and corrosion resistance, thus extend their service life in harsh environments [38, 105, 139–145]. Among the techniques, laser remelting treatments have been performed with different laser sources. For example, Sun et al. [105] and Amaya et al. [38, 139] observed that the microstructural transformation of the commercially pure titanium alloy (grade 2) from the α phase to acicular martensite significantly enhances the corrosion resistance in NaCl solutions during laser remelting treatment. However, the laser remelting treatments do not seem to alter the corrosion resistance of the Ti6Al4V specimens significantly, because they do not produce phase transformations [38]. In comparison, the pitting corrosion resistance of laser-treated Ti6Al4V samples in NaCl and Hank's solutions under the influence of argon and nitrogen-shielding gases was investigated using excimer laser [140]. The excimer surface treatment was reported to improve the pitting potential particularly under argon shielding. Garcia et al. [143] reported that laser remelting treatment of Ti-6Al-4V and commercially pure Ti in a nitrogen atmosphere produces sufficiently dense and defect-free TiN coatings which improved the corrosion resistance of the Ti alloys.

On the other hand, Zhu et al. [145], studied the effect of cryo-treatment on corrosion behavior and mechanical properties of laser-welded commercial pure titanium in an artificial saliva solution (0.4 NaCl, 0.4 KCl, 0.795 $CaCl_2{\cdot}2H_2O$, 0.78 $NaH_2PO4{\cdot}2H_2O$, 0.005 $Na_2S{\cdot}2H_2O$, 1.0 $CO(NH_2)_2$). The results showed that the laser-welded titanium after cryo-treatment has the highest passivation behavior. The authors also found that both the tensile strength and the elongation of titanium and laser-welded titanium could be improved by cryo-treatment without affecting its corrosion resistance.

5 Laser welding of titanium to other alloys

Recently, hybrid structures of dissimilar joints between different titanium alloys as well as titanium and other lightweight alloys such as Ti/Al, Ti/Mg, and Ti/Ti and even with harder alloys such as steels are widely used for many applications, in

order to improve performance, cost-effectiveness, and to exploit the advantages of different materials. Thus, it is important to understand the joining mechanism and performance of titanium to other metal dissimilar joints. However, joining of dissimilar materials is challenging largely due to large differences in physical and metallurgical properties. Table 1 compares the most significant room temperature physical properties of Ti, Al, Mg, Ni, and Fe [5, 53, 101, 146]. Over the years, varieties of titanium/other metals have been joined by laser welding under optimized processing conditions. In this section, the potential of several laser-welding techniques for joining titanium to other alloys is reviewed.

5.1 Ti/Ti dissimilar alloys

Recently, efforts have been intensified in developing high temperature titanium intermetallic for high temperature services, in particular, Ti_2AlNb-based alloys containing the orthorhombic O phase have received wide attention as potential materials for aircraft engine because of their high fracture toughness, high specific strength, and room temperature ductility [147, 148]. Hybrid structures made from the Ti_2AlNb-based and conventional titanium dissimilar alloys are often used for the critical parts of some aircraft engines [110]. Thus, the establishment of the most suitable joining techniques for Ti_2AlNb-based to conventional titanium alloys is essential [110, 149, 150]. Despite the lack of suitable filler metals for the titanium aluminides which hindered its wide applications [151], some work exists on the laser welding process for Ti_2AlNb-based to titanium dissimilar alloys including Ti-22Al-27Nb/TC4 [110], Ti-22Al-25Nb/TA15 [150, 152], BTi-6431S/TA15 [153], and Ti–22Al–27Nb/TA15 (laser-TIG hybrid) [154]. So far, most of the work focused mainly on microstructure and mechanical properties. The microstructural evolution of the laser-welded Ti_2AlNb-based alloys to other titanium alloys joints revealed that the single B2 phase is easily formed in the FZ, which degrades the weld performance [110, 150, 152–154]. For instance, Lie et al. [110] studied the microstructural evolution and mechanical properties of laser-welded Ti-22Al-27Nb/Ti-6Al-4V dissimilar joints. The weld metal was composed of mainly B2 and martensitic α' due to the high cooling rate and the uneven distribution of the β phase stabilizer. Furthermore, the phase composition in the HAZ varied with thermal cycles during welding. The presence of the B2 and the martensitic α' phases in weld improved the tensile strength up to 1043 MPa, about 92% of the Ti6Al4V alloy, but the ductility dropped sharply to only 5.65%. A similar trend was observed for Ti-22Al-25Nb/TA15 dissimilar alloys [150]. In both cases, a twinned slip system was considered the main reason for the rapid drop of the ductility in the FZ [110, 150]. Shen et al. [152] joined 22Al-25Nb/TA15 dissimilar titanium alloys under single and dual beam. It was found that a single B2 phase was formed in the FZ during the single mode because of the β stabilizer and rapid cooling rate of the laser welding, while B2 and O phases were observed during the dual mode process because of the decrease in the cooling rate. The formation of the hard O phase in the FZ during the dual mode increased the average tensile strength of the welded joints from 943.2 to 1011 MPa. Furthermore, the elongation was increased from 3.56 to 5.67% due to the deeper and evener dimple compared to the single mode process.

Table 2 compares the joint strength of Ti/Ti dissimilar joints under different laser welding conditions. The comparison of the dissimilar joints tensile strength shows that the

Table 1 Room temperature physical properties of Ti, Fe, Al, Mg, and Ni [53, 101, 146]

Properties	Unit	Titanium	Iron	Aluminum	Nickel	Magnesium
Ionization energy	eV	6.8	7.8	6	7.6	7.6
Specific heat	J/kg/K	519	795	1080	460	1360
Latent heat of fusion	kJ/kg	419	272	398	297	368
Melting point	°C	1667	1536	660	1455	650
Boiling point	°C	3285	2860	2520	2730	1090
Viscosity	kg/m/s	0.0052	0.0055	0.0013	0.0049	0.00125
Surface tension	N/m	1.65	1.872	0.914	1.778	0.559
Thermal conductivity	W/m/K	22	38	238	88.5	78
Thermal diffusivity	m^2/s	2.15×10^{-6}	6.80×10^{-6}	3.65×10^{-5}	22.66×10^{-6}	3.73×10^{-5}
Coefficient of thermal expansion	1/K	8.9×10^{-6}	10×10^{-6}	24×10^{-6}	13.3×10^{-6}	25×10^{-6}
Density	kg/m^3	4500	7015	2385	8900	1590
Elastic modulus	N/m^3	10.3×10^{10}	21×10^{10}	7.06×10^{10}	19.3×10^{10}	4.47×10^{10}
Electrical resistivity	μΩm	0.4	1.386	0.2425	0.72	0.274

Table 2 Comparison of the joint strength of Ti/Ti dissimilar joints under different laser welding conditions

Laser heat source	Materials	Thickness	Joint design	Joint strength (MPa)	Reference
CO_2 laser	Ti-22Al-27Nb/TC4	2.5 mm both	Butt	1043	[110]
Pulse YAG laser	BTi-6431S/TA15	2 mm both	Butt	1113 and 490 @ 550 °C	[153]
CO_2 laser-TIG hybrid	Ti-22Al-25Nb/TA15	2.5 mm both	Butt	905.9 and 424.8 @ 650 °C	[154]
Nd:YAG	Ti-22Al-25Nb/TA15	1 mm both	Butt	1019 and 714 at (500 °C)	[150]
Single and dual LBW Nd:YAG	Ti-22Al-25Nb/TA15	2 mm both	Butt	Single (943.2) dual (1011) at 550 °C Single (663) dual (655)	[152]

tensile behavior of the welded joints depends largely on the phase compositions. Furthermore, the results of these studies confirmed that joint performance is significantly influenced by temperature.

5.2 Ti/steel

Steel is currently the structural material of choice, due to their inherent properties, including high strength and toughness, good ductility, and low cost. With the expanding use of Ti, there is considerable interest in joining Ti with steel as these joints have many applications [155, 156]. Nevertheless, the dissimilar joining of Ti with steels is very difficult due to the limited mutual solubility of Ti and Fe in the solid state [157] and the wide difference in the coefficient of linear expansion develops strain at the bond interface of the dissimilar metals [158]. When Ti is joined with steel, brittle Ti-based intermetallic phases, such as Ti_xFe_y, Ti_xNi_y, and Ti_xCr_y, are readily produced and, hence, the bonding strength significantly deteriorated [155, 159–164]. Therefore, suppressing the formation of hard and brittle IMCs is the key to obtaining a reliable joint.

5.2.1 Autogenous laser welding of Ti/steel

An autogenous laser welding would not usually be expected to produce joint with good mechanical resistance. However, autogenous lap welding has been reported with a joint strength of up to 190 MPa [156, 161]. Zhao et al. [161] studied the performance of laser-welded Ti-6Al-4V/42CrMo dissimilar alloys using experimental and numerical simulation. The analysis interface characteristics showed that TiFe and $TiFe_2$ intermetallic phases were observed at the Ti interface and that the thickness of the IMC layer depends largely on the heat input. The authors suggested that the IMCs could be suppressed by optimizing the laser output parameters.

Similarly, laser-welded titanium to steel dissimilar joints without transition material in butt design was also reported in the literature. Generally, laser beam offset toward the steel is considered as the best way to suppress liquid mixing of the base metals during welding [162–166]. For example, Satoh et al. [166] reported the feasibility of joining titanium to stainless steel without filler material using Nd:YAG laser. Hard and brittle IMCs readily formed at the Ti interface, because the liquid state mixing between the titanium alloy and the steel is not fully suppressed. Chen et al. [162] critically observed the effect of laser beam offsetting on microstructural characteristic and fracture behavior of Ti-6Al-4V/201 stainless steel joints with 1-mm thickness each using CO_2 laser. The authors suggested that laser beam offset toward the stainless steel is the best way to suppress the liquid mixing during welding. The IMC layers of FeTi + α-Ti and FeTi + Fe_2Ti + $Ti_5Fe_{17}Cr_5$ were formed with uniform thickness along the interface. Under optimized processing conditions, a joint strength of up to 150 MPa was obtained.

5.2.2 Ti/steel with interlayer

As mentioned in Sect. 5.2, autogenous welding of titanium to steel alloys resulted in the formation of IMCs, which degraded the joint performance. Several works suggested that one way to improve the joints quality is to modify the composition of the FZ using interlayer, which is compatible with the BM [159, 167–169]. Generally, titanium demonstrates good weldability with very few metals (beta isomorphous elements) which do not form IMCs with it, such as zirconium, niobium, molybdenum, tantalum, vanadium, and hafnium. The use of these elements as interlayers improves the mechanical performance of titanium to steel joints [165, 170, 171].

Taking vanadium (V) into consideration as an interlayer between the titanium and the steel, because V has 100% solubility Ti also the Fe-V system also shows large continuous solid solutions. Thus, V-based foil is a good choice for use as transition material for Ti/steel dissimilar joints [165, 170]. The earlier attempt to used V and Ta as interlayers between the titanium and the steel alloys under keyhole mode using CO_2 laser was not successful due to oxidation and brittle phases developed [165]. However, Tomashchuk et al. [170] reported a successful Ti-6Al-4V/AISI 316L dissimilar joint via pure V interlayer using continuous wave Yb:YAG laser. The authors observed that two-pass welding give the best joint quality and

high strength (367 MPa). Interestingly, because of the rapid cooling rates of the laser welding process, the brittle σ-phase between the Fe and the V was suppressed.

Tantalum (Ta), on the other hand, has 100% solubility in titanium and sufficiently good solubility with the Fe, Cr, and Ni. Although the earlier attempt to used pure Ta as interlayer failed due to oxidation problem, a joint strength of about 40 MPa was reported [165].

The use of niobium (Nb) as an interlayer for titanium to steel dissimilar joint has also been reported in the literature. Generally, Nb melts at 2467 °C which is very high as compared to the melting point of Ti and Fe (Table 1); Nb and Ti form a complete solid solution throughout the range of composition [101]. Zhang et al. [171] studied pulsed laser-welded Ti6Al4V/301L dissimilar joint via pure Nb plate using a hybrid joining mechanism (fusion welding at Ti-Nb interface and diffusion bonding at the Nb-Steel interface). The reaction layers of Fe_7Nb_6, Fe_2Nb, and α-Fe were observed at the Nb-steel interface. The joint fractured at the reaction layer with a strength of about 370 MPa.

Although zirconium, niobium, molybdenum, tantalum, vanadium, and hafnium interlayers could suppress the formation of brittle Ti-Fe IMCs, their cost is high. Therefore, cheaper and more available interlayers such as copper and nickel have been considered as potential interlayers for Ti alloys to steel joints [159, 167]. Many researchers have explored the use of copper as potential interlayer for titanium and steel dissimilar joint, because copper does not form IMCs with Fe and Ti-Cu IMCs are less brittle than the Ti-Fe IMCs [35, 159, 172–175]. For example, Tomashchuk et al. [159] laser-welded Ti6Al4V/AISI 316L using pure Cu interlayer. It was found that under optimum parameters, a joint with strength of 359 MPa was obtained and a $CuTi_2$ + FeTi + α-Ti layer near the solid titanium alloy was observed. Similarly, Groza et al. [174] and Mitelea et al. [172] investigated laser-welded Ti6Al4V/X5CrNi18 dissimilar joint using 600-μm copper foil by continuous wave Nd:YAG laser. Laser beam offset to the Cu-steel interface minimized the melting of the titanium alloy and improved the weld strength (400 MPa).

The results of these studies suggested that Cu-based foil improved the metallurgical reaction of the titanium to steel joints to some extent. However, the risk of oxidation and the brittle IMC formation is still not resolved even with optimization of the welding parameters; the titanium to copper interfacial joint remains the weakest part of the joint. According to the Fe-Cu-Ti ternary diagram, copper containing phases has low temperature stability because of the copper containing phases has low temperature transformation [176]. Therefore, Gao et al. [177] studied the feasibility of improving the stability and efficiency associated with high reflection of laser beam of copper containing phases for Ti6Al4V/AISI 316 dissimilar joints with Cu3Si wire using laser-arc hybrid welding. It was found that under appropriate parameters, a joint with mechanical resistance of about 212 MPa was achieved. In another study, the use of a composite insert obtained by means of explosive welding of four sheets (VT1-0 titanium, high-purity tantalum, pure copper (M1), and 12Kh18N10T steel) for VT1-0 titanium alloy to 12Kh18N10T stainless steel dissimilar joints was studied with subsequent butt-end laser welding of similar metals using CO_2 laser [164]. The results of the metallographic and spectrographic investigations showed that the composite fractured over the copper layer, with the highest strength of 417 MPa.

Using Mg as interlayer elements for Ti alloys/steel was also reported in the literature, Mg could not mix with both Ti and Fe in the liquid state at ambient pressure. In addition, it would not react with Ti or Fe to form IMCs [178]. Thus, Mg is chosen as an interlayer for Ti/Steel joints. Gao et al. [179] studied fiber laser-welded Ti6Al4V/AISI 304L dissimilar joint using pure Mg foil interlayer. It was found that at high laser power > 2.5kW, the fracture changes from steel/weld interface to the titanium/weld interface. An acceptable joint with cross-weld tensile strength of 221 MPa was achieved. The authors suggested that the laser power and the differences in thermal conductivity of Ti6Al4V and AISI 304L play a big role in the joining mechanisms of Ti6Al4V and AISI 304L joint using Mg interlayer [179].

Table 3 compares the joint strength of Ti/steel dissimilar joints under different laser welding conditions. Based on the existing literature, the interfacial characteristics and joint performances in Ti alloys to steel joints produced using laser beam welding process with and without the addition of interlayers were investigated. The benefits of using Cu, Nb, V, Mg, and Ta as transition materials were also explored. The presence of interlayer was essential for successful joining Ti to steel. To further enhance the reliability of the joint and improve its performance, the possibility of using more interlayers should be explored. A comparison of the joints mechanical properties shows that relatively good static strength has been achieved with the insertion of Cu and Nb intermediate elements. However, no study has focused on the fatigue and corrosion behavior of the joints parts.

5.3 Ti/Al alloys

Aluminum and its alloys are one of the most widely used construction materials because of its excellent combination of properties such as high strength to weight ratio and superior corrosion resistance. Recently, the application of titanium to aluminum hybrid structures has grown particularly in automotive and aerospace industries. However, joining titanium to aluminum is challenging due to their wide physical and metallurgical properties differences. According to an Ti-Al equilibrium phase diagram [180], Ti and Al IMCs such as Ti_3Al, TiAl, $TiAl_2$, and $TiAl_3$ are easily formed in the weld FZ and several IMCs especially $TiAl_2$ and $TiAl_3$ lead to weld defects

Table 3 Comparison of the joint strength of Ti/steel dissimilar joints under different laser welding conditions

Laser heat source	Materials	Thickness	Joint design	Transition material	Joint strength (MPa)	Reference
CW Nd:YAG laser	Ti6Al4V/42CrMo	1 mm/Ti6Al4V and 2 mm/42CrMo	Lap	No transition material	Not reported	[161]
PW Nd:YAG laser	CP-Ti Gr2/SUS304	0.4 mm/SUS304 and 0.3 mm/CP-Ti	Lap	No transition material	190	[156]
PW Nd:YAG laser	CP-Ti Gr2/316 steel	0.8 mm both	Butt	No transition material	153.9	[166]
CO_2 laser	Ti6Al4V/201 SS	1 mm both	Butt	No transition material	150	[162]
CW Nd:YAG laser	Ti6Al4V/X5CrNi18-10	2 mm both	Butt	Cu foil 600-μm thick	400	[172, 174]
CW Nd:YAG laser	12Kh18N10T (AISI 321)/VT1-0 (grade 2)	2 mm both	Butt	Cu (1-mm thick)	474	[175]
PW Nd:YAG laser	TC4/SUS301L	0.8 mm both	Butt	Cu (0.4-mm thick)	350	[35]
Fiber laser-arc hybrid	Ti6Al4V/AISI316L	2 mm both	Butt	Cu3Si wire	212	[177]
Fiber laser	Ti6Al4V/AISI304L	2 mm both	Butt	AZ31B Mg wire (1-mm thick)	221	[179]
CW CO_2 laser	CP Ti/SS 304	3 mm both	Butt	Pure Ta strip (0.5-mm thick)	44	[165]
CW Yb:YAG	Ti6Al4V/AISI316L	2 mm both	Butt	Pure V foil (1-mm thick)	367	[170]
Nd:YAG fiber laser	Ti6Al4V/AISI301L	0.8 mm both	Butt	Pure Nb (1-mm thick)	370	[171]
CO_2 laser	VT1-0/12Kh18N10T stainless steel	3 mm both	Butt	VT1-0-Ta-Cu-12Kh18N10T	417	[164]

[146, 181–188]. Thus, fusion welding of titanium and aluminum has a metallurgical challenge due to the unavoidable formation of brittle IMCs. It is necessary to suppress the formation and growth of Ti and Al IMCs [36, 186]. However, if Ti/Al dissimilar joints with high strength and toughness is required, the IMC layers has to be limited to a maximum thickness of less than 10 μm.

5.3.1 Ti/Al dissimilar joining using keyhole laser welding

Despite the difficulties in minimizing the mixing between the melted titanium and aluminum alloys at typical welding temperature, laser welding of Ti/Al dissimilar joint in keyhole mode was reported [170, 181, 188–191]. The keyhole welding process provides good flexibility and controllability. In addition, keyhole laser welding has high welding speed, which limits the metallurgical reaction time [192]. Thus, the formation of the brittle IMCs may be suppressed using this welding technique. For butt joint design, laser beam offset is considered as the main parameter to control the IMCs thickness. Many authors suggested laser beam offset on the titanium side such that the Al/weld joining is achieved by conduction [181, 188, 189]. For instance, Kreimeyer et al. [189] studied the properties of CO_2 laser-welded 1.15-mm-thick AA6016T4 to 0.8-mm Ti6Al4V alloys using CP-Ti (grade 2) wire. It was found that the beam offset at 0.3 mm on the Ti side minimized the melting of the Al, which enhanced the joint static strength (200 MPa). Under optimum parameters, the IMC layer thickness was minimized to less than 2 μm as shown in Fig. 10. In addition, the growth of the intermetallic phase has only minor dependence on the energy input per unit length due to limited diffusibility of Al in titanium aluminide phases. Mujamdar et al. [181] studied laser-welded Ti6Al4V to wrought Al alloy (Al-1Mg-0.9Si) with 3-mm thickness both using CO_2 laser with and without Nb foil. It was found that with laser beam offset on the Ti side, TiAl, and Al_3Ti brittle phases were observed. However, when Nb foil was added as a buffer between the Ti and the Al, the Ti-Al IMCs were removed and the joint strength increased from 57 to 120 MPa. Recently, Casalino [188] studied laser-welded 1.5-mm-thick Ti6Al4V/AA5754 dissimilar joint using fiber laser offset welding with keyhole made entirely on the titanium side. It was found that under optimum parameters (0.75 mm beam offset and 50 J/mm linear energy), the thickness of the IMC layer was limited to less than 1 μm and the ultimate tensile strength of 191 MPa was obtained.

Some work has also been conducted on titanium overlap on aluminum [185, 186, 192]. Lee et al. [185, 186] welded CP-Ti to A1050 using single mode fiber laser. It was observed that high welding speed (50 m/min) at 1 kW laser power significantly reduced the IMC layer thickness. However, narrow width joint was observed which affects the load capacity of the joint. Chen et al. [192] investigated the feasibility of improving the load capacity of the Ti6Al4V-on-5052 Al alloy overlap joints using multimode keyhole laser welding. It was found that the tensile capacity of the joint increases firstly and then decreases with increasing laser power or decreasing welding speed. The decrease in tensile capacity observed

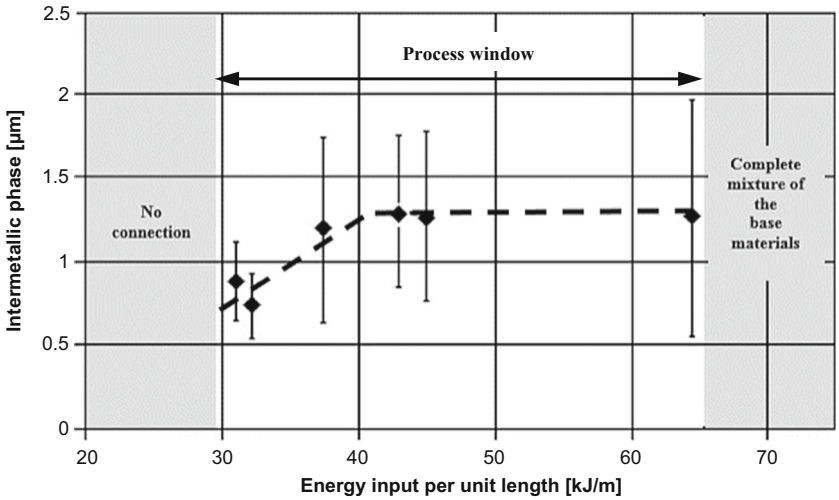

Fig. 10 Process window for laser-welded AA6016T4/Ti6Al4V tailored blanks [189]

was associated with deep underfill and mass formation of IMCs when the laser power increases or welding speed decreases. The results of this study suggested that the weld geometry could be regulated by precise control of the welding processing parameters. Generally, for keyhole laser-welded Ti/Al alloys, enhancing the stability of the keyhole continues to be the principal challenge.

5.3.2 Ti/Al dissimilar joining using laser welding-brazing method

A considerable number of studies focused on titanium to aluminum dissimilar joining based on laser-brazing approach such that the laser irradiates on the Al that melts and wets the solid Ti surface [36, 189, 193–196]. During laser welding-brazing (LWB), the thickness of the IMCs can be limited to few microns, which greatly improve the mechanical properties of the joint.

Therefore, many previous works have been performed to control the thickness of the IMCs using filler wire containing high silicon content, which changes the intermetallic phase type and significantly depressed the growth of the IMC layer [195, 196]. Chen et al. [36, 194, 197] joined Ti6Al4V to 5A06Al dissimilar joints using laser welding-brazing approach with an AlSi12 filler wire. The results showed that thin interfacial reaction layer with thickness of less 1 μm on the titanium-brazed side composed of $Ti_7Al_5Si_{12}$ and $TiAl_3$ under optimum processing parameters was observed [195]. Peyre et al. [196] laser-welded Ti6Al4V to A5754 alloy with 1.5-mm thickness in overlap configuration using AlSi12 filler. It was observed that the process parameters did not play a significant role on mechanical strength, which reached 120 MPa.

Some authors focused on the improvement of the joint performance by modifying the interfacial reaction non-homogeneity and improve the spreadability of liquid metal using rectangular spot laser beam with suitable welding groove or U-slot to increase the length of the Ti/Al interface [182, 183, 198, 199]. For instance, Vaidya et al. [182] studied 1.8-mm-thick Ti6Al4V/2-mm AA6056-T6 dissimilar butt joined with chamfered titanium alloy inserted into the profiled aluminum alloy such that only the aluminum melted during the split beam Nd:YAG welding. Under optimum welding conditions, the length of the Al/Ti interface and thickness of the interfacial reaction layer were reduced. The joint strength reached 255 MPa, about 65% of the AA6056-T6 BM. Chen et al. [199] studied effect of the rectangular laser spot on the dissimilar assembly of 1.5-mm-thick Ti6Al4V to 1.5-mm 5A06 with V-shaped groove and AlSi12 filler wire. It was found that the rectangular laser spot with V-shaped groove on the BM improved the homogenization of the interfacial reaction layer and the average tensile strength reaches 278 MPa under optimized parameters.

Some works concentrated on the improvement of the joint performance via fiber laser brazing with beam offset on Al and without groove preparation or filler metal [190, 191]. Song et al. [190] studied the effect of laser beam offset on the Ti/Al IMC thickness for laser-welded Ti6Al4V/A6061-T6. It was found that under optimum processing conditions (1 mm offset laser beam offset on the Al side, 4 kW, and 4 m/min), the IMC layer thickness was limited to only 0.26 μm, which improved the joint tensile strength to 203 MPa. Tomashchuk et al. [191] laser welded Ti6Al4V/AA5754 and reported that high linear energy of the welding ≥ 37.5 kJ/m and 0.2-mm beam offset toward the Al promoted the formation of thin (< 20 μm) TiAl IMC at the interface, which improved the joint ultimate tensile strength (120 MPa). Recently, Sahul et al. [187] investigated CP-Ti (grade 2)/5083 dissimilar joints produced by laser welding-brazing method using 1.2-mm 5087 (AlMg4.5MnZr) filler wire. The results showed that with the use of Al-based filler, no reduction in the weld thickness was observed as reported by Tomashchuk et al. [191]. The joint with highest strength (180 MPa) was obtained at 300 μm laser beam offset on the Al side.

An important consideration for the laser beam offset on the Al is the tilt of the laser head is crucial to minimize the

reflection of the laser beam due to the low laser beam absorption of the aluminum alloy [200]. Gao et al. [201] investigated the feasibility of improving the high reflection of the laser beam by the Al alloy with aid of arc preheating of the BM. In a study of Ti6Al4V/AA6061 dissimilar joints using fiber laser-cold metal transfer arc (laser-CMT) hybrid welding. It was observed that at optimum heat input (83–98 J/mm), the cross-weld tensile strength of the joints is up to 213 MPa. The IMC layer of the accepted joint is usually thin and continuous and consists of only $TiAl_2$ due to fast solidification rate.

Generally, the LWB significantly suppressed the formation IMCs, which in turn improved the joint mechanical resistance. However, the major drawbacks with this approach are the poor wetting and spreading, which significantly affect the weld appearance and the process stability.

Table 4 compares the joint strength of Ti/Al dissimilar joints under different laser welding conditions. It can be seen that many works adopted various techniques to improve the joint strength. These efforts result in the static strength increase of laser-welded Ti/Al joints, but the tensile strength of the joint is still at the level of about 60–70% of the Al alloy BM. Therefore, more research efforts are required on the formation mechanism of the IMCs.

5.4 Ti/Mg alloys

Magnesium being the lightest structural metal receives great attention particularly in automotive and aerospace industries because of its low density, high strength to weight ratio, good formability, and easy recyclability. However, its application is often restricted by its relatively poor corrosion resistance [4, 37, 202]. Therefore, joining titanium to magnesium would be an excellent combination for many industrial applications. However, joining magnesium to titanium is quite challenging because of the notable mismatch in physical and mechanical properties and lack of metallurgical compatibility [37, 89, 203, 204].

The literature shows that despite magnesium and titanium are immiscible, metallurgical bonding was achieved using a transition material, which is compatible with both base materials. The dissolution and diffusion of the filler material produced an intermetallic phase (IMC) with the titanium base metal substrate when locally experienced high temperature. The formation of these IMCs along the Mg-Ti alloy interface can facilitate metallurgical bonding between the magnesium alloy and the titanium, but they can also be detrimental for mechanical performance of the joints [37, 89, 203, 204]. For instance, Gao et al. [203, 204] investigated the process parameters, properties, and bonding mechanism of AZ31B/Ti-6Al-4V laser-welded joints using AZ31 filler wire or melting of thicker Mg base metal to achieve bonding. It was found that laser beam offset significantly influences the bonding mechanism and the joint performance. Under optimum laser beam offset 0.3–0.4 mm, the intermixing of the molten titanium with liquid magnesium during the keyhole welding caused the formation of lamellar and granular mixtures of titanium and aluminum element in the fusion zone, which significantly improved the joints tensile strength (266 MPa) [203]. In

Table 4 Comparison of the joint strength of Ti/Al dissimilar joints under different laser welding conditions

Laser heat source	Materials	Thickness	Joint design	Transition material	Joint strength (MPa)	Reference
CO_2 laser	AA6016T4/Ti6Al4V	TC4 0.8 mm/AA6016 1.15 mm	Butt	CP-Ti filler	200	[189]
CO_2 laser	TiA16V4/Al-1 wt% Mg-0.9 wt% Si	3 mm both	Butt	No transition material	57	[181]
CO_2 laser	TiA16V4/Al-1 wt% Mg-0.9 wt% Si	3 mm both	Butt	Nb plate	120	[181]
CO_2 laser	Ti-6Al-4V/AA6056-T6	1.5 mm Ti-6Al-4V/2 mm AA6056-T6	Butt	AlSi12 filler	255	[182]
Rectangular spot laser	Ti6Al4V/5A06	1.5 mm both	Butt	AlSi12 filler	278	[199]
single-mode fiber laser	CP-Ti/A1050	0.3 mm both	Lap	No transition material	350	[185, 186]
Multimode CO_2 laser	Ti-6Al-4V/5052	Ti-6Al-4V (1 mm)/5052 (2 mm)	Lap	No transition material	184	[192]
Yb:YAG disk laser	T40/A5754	1.5 mm both	Lap	Al5Si filler wire	120	[196]
Yb:YAG laser	Ti6Al4V/AA5754	2 mm both	Butt	No transition material	120	[191]
Yb:YAG laser	T40/5754Al	1.5 mm both	Butt	No transition material	191	[188]
Hybrid-fiber laser and CMT welder	Ti-6Al-4V/AA6061	2 mm both	Butt	Al-12Si wire	213	[201]
CW disk laser weld brazing	5083/CP-Ti (grade 2)	2 mm both	Butt	5087 filler wire	180	[187]

another study, Tan et al. [89, 90] investigated the Ti6Al4V/AZ31B lap joints both with thickness of 1.5 mm produced using laser welding-brazing with addition of Al element into 1.2-mm diameter Mg-based filler wire. The results have shown that with the increasing content of aluminum element, metallurgical bonding was achieved due to the formation of Ti_3Al interfacial reaction layer with maximum thickness of 1.5 μm compared to mechanical bonding by direct joining or using a filler wire with low aluminum content. The Ti_3Al IMC layer prevented crack propagation and enhanced the joints strength from 25.5 ± 5.5 to 2057 N through precipitation strengthening [89]. To further improve the interfacial bonding between the immiscible Mg and Ti, the use of electrodeposited Ni- [37] and Cu-coated [205] interlayers have been used by Tan and co-workers. For AZ31B to Ni-coated Ti6Al4V joints, a formation of Ti_3Al phase was observed at the direct irradiation zone and Al-Ni phase, Mg-Al-Ni ternary compound adjacent to the FZ at the intermediate zone. The joint tensile shear peak load of 2387 N was obtained under optimized processing conditions. The influence of the laser power on the AZ31B to Cu-coated Ti6Al4V revealed that the brazed interface consists of Ti_3Al phase produced at direct irradiation zone, $Ti_2(Cu, Al)$ formed at intermediate zone and (α-Mg + Mg_2Cu) eutectic structure formed at the seam head zone. The joint tensile shear peak load of 2314 N was obtained at the laser power of 1300 W. The results of these studies suggested that the addition of Ni and Cu improved the spreadability of the molten filler on the Ti plate.

Table 5 compares the joint strength of Ti/Mg dissimilar joints under different laser welding conditions. Based on the existing literature, the interfacial characteristics and the mechanism of wetting in Mg alloys to Ti joints produced using laser process with addition of interlayers were investigated. The feasibility of using Al, Ni, and Cu intermediate elements was also explored. The selection of suitable interlayer is crucial for successful bonding of Mg to Ti. A comparison of the joints properties reveals that relatively good static strength about 88% of the Mg alloy BM has been achieved [37]. To improve the joints performance, the analysis of the morphology characteristic, microstructure, and mechanical properties of the Mg/Ti welded joints under single-beam and dual-beam laser welding-brazing methods with addition various interlayers that form eutectic with Mg such as Ag, Sn, Al-Cu, and Ag-Sn should be explored. In addition, research efforts are also needed on the fatigue and corrosion behavior of the joints parts.

6 Residual stresses in laser welding of titanium and its alloys

Residual stresses are always observed in the laser titanium alloys welds because of the differential cooling rates, the plastic flow, and the allotropic phase transformations with volume changes. These residual stresses caused distortions, deteriorate the mechanical performance, especially the fatigue strength, and fracture toughness. Considering the possible aerospace applications of titanium alloys, the investigations of the residual distribution are essential. Generally, the residual stresses distribution in the laser welding is complex and non-uniform [14, 18, 62, 206–208]. For instance, during welding, both the base and the weld metals experience severe thermal cycle leading to generation of residual stresses [207]. It is worth noting that the residual stresses and deformations are generally influence by joint design, joining techniques, metallurgical properties, and heat input [209]. Many works suggested that laser beam welding techniques proved to be more feasible for production of titanium alloys joints [13, 18, 104, 210]. Zhang et al. [18] studied the residual stress distribution of BT20 and Ti6Al4V alloys welded by CO_2 laser beam and tungsten inert gas using hole drill method (HDM). The results showed that the distributions of residual stresses in CO_2 laser welding is similar to that obtained from the joint welded by TIG. However, the residual stresses in the HAZ are about 100 MPa lower for laser welding than for TIG welding due narrower weld seam. In contrast, Chuan et al. [210] carried out finite elements simulations on 4-mm-thick Ti-6Al-4V alloy and reported that the residual stresses are not uniform. The

Table 5 Comparison of the joint strength of Ti/Mg dissimilar joints under different laser welding conditions

Laser heat source	Materials	Thickness	Joint design	Transition material	Joint strength (MPa)/shear load (N)	Reference
Fiber laser	Ti-6Al-4V/AZ31B	2 mm both	Butt	AZ31B Mg filler (1 mm dia)	200.3 MPa	[204]
Keyhole fiber laser	Ti-6Al-4V/AZ31B-T5	2 mm Ti-6Al-4V and 3 mm AZ31B-T5	Butt	No transition material	266 MPa	[203]
Laser welding-brazing	Ti6Al4V/AZ31B	1.5 mm both	Lap	AZ31 filler	1049 ± 227 N	[89]
Laser welding-brazing	Ti6Al4V/AZ31B	1.5 mm both	Lap	AZ91 filler Mg (1.2 mm dia)	2057 N	[90]
Laser welding-brazing	Ti6Al4V/AZ31B	1 mm both	Lap	Ni coating (1.9 ± 0.5 μm)	2387 N	[37]
Laser welding-brazing	Ti6Al4V/AZ31B	1.2 mm both	Lap	Cu coating (12.8 ± 1.0 μm)	2314 N	[205]

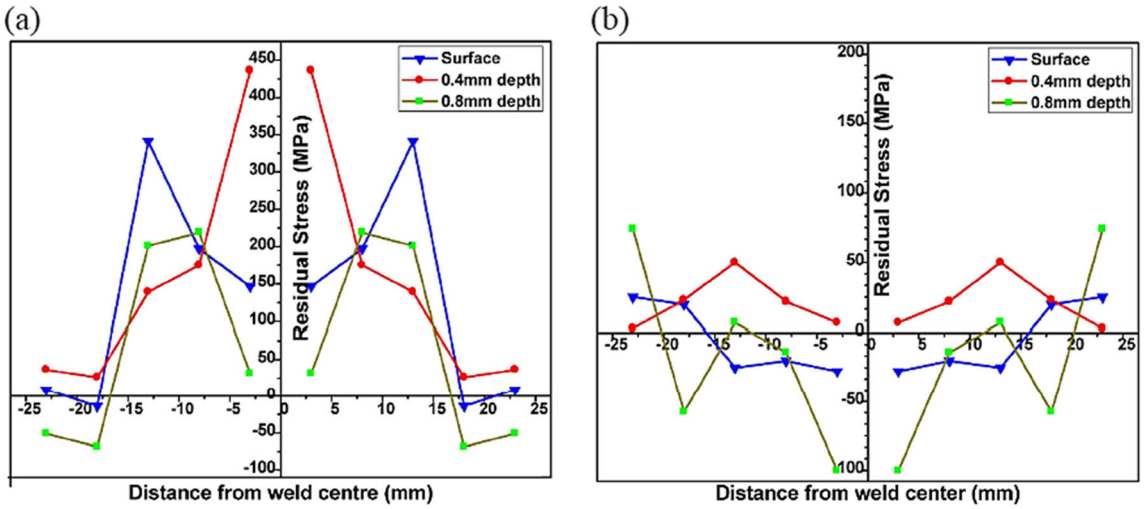

Fig. 11 Longitudinal residual stress distribution showing **a** pulsed tungsten inert gas and **b** pulsed laser-welded Ti5Al2.5Sn joints [62]

discrepancies of these findings are mainly due to non-uniform expansion and contraction resulted from welding process. Gao et al. [13] also reported that compared with TIG welding, pulsed Nd:YAG laser welding on Ti6Al4V produced less residual stresses, lower heat input, less deformation, narrower weld bead, and narrower HAZ. Recently, Junaid et al. [62] studied the residual stress distribution of pulsed laser-welded and pulsed tungsten inert gas welded Ti5Al2.5Sn alloy using speed hole drilling strain measurement. Figure 11 shows their residual stress distribution. For pulsed tungsten inert gas welded joints (Fig 11a), the maximum tensile residual stress of 430 MPa was found at a distance of 3 mm from the centerline. Whereas, for laser-welded joints, compressive stress of 100 MPa at 3 mm from the centerline was reported.

To relieve the residual stresses, it is recommended that the laser-processed titanium alloys be annealed at 600 °C for 2 h in a vacuum environment; this enables the decrease of the welding residual stresses by almost 90% [18]. Fomin et al. [33] studied the influence of post weld heat treatment (PWHT) on the residual stresses of 2.6-mm-thick CW ytterbium fiber laser-welded Ti6Al4V using HDM. The longitudinal and transverse residual stresses distribution of the weld is shown in Fig. 12a. It can be seen that after annealing at 540 °C, relief the stress from 650 to 90 MPa, whereas, post weld heating at 750 °C relieved almost all the stress (Fig. 12b).

7 Post weld heat treatment

In titanium alloys, a required mechanical performance could be obtained by controlling microstructure. Post weld heat treatment results in the transform the weld zone microstructure can serve as viable option to achieved improved mechanical properties [7, 18, 33, 82, 211]. Kabir et al. [64] laser welded Ti6Al4V alloy and reported that full hardness and desired mechanical properties are achieved after subsequent full annealing and aging treatment after welding. The increase in hardness has been attributed to the decomposition of martensitic α' structure into an equilibrium lamellar α+β structure. Recently, Fomin et al. [33] studied the effect of the PWHT on the 2.6-mm-thick Ti6Al4V butt joints produced by CW ytterbium fiber laser. It was observed that PWHT at high annealing

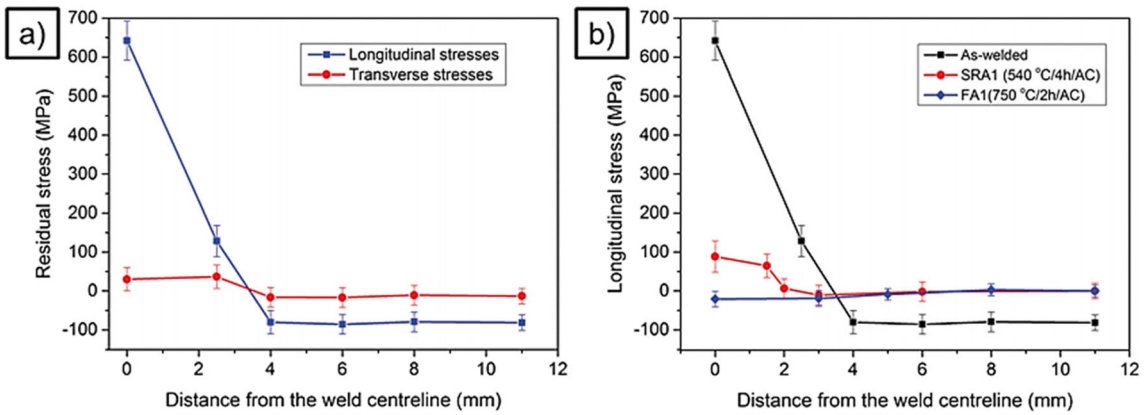

Fig. 12 **a** Longitudinal and transverse residual stresses distribution of the Ti6Al4V butt weld. **b** Influence of PWHT on the longitudinal residual stresses [33]

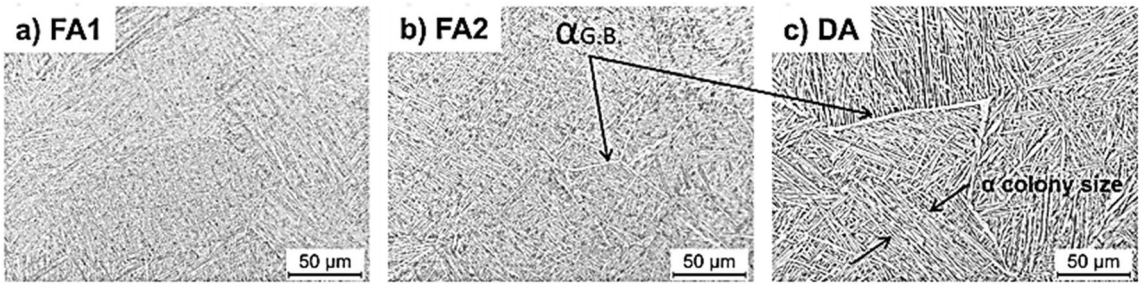

Fig. 13 Effect of PWHT on the microstructure of Ti6Al4V alloy: **a** Full annealing (FA1) at 750 °C/2h/AC, **b** full annealing (FA2) at 850 °C/1h/AC, **c** duplex annealing (DA) at 920 °C/45 min/AC + 540 °C/4h/AC [33]

temperatures (above 750 °C) resulted in transformation of fine martensitic structure into more ductile coarse lamellar in the weld zone as shown in Fig. 13, which enhanced the fatigue performance of the joint (Fig. 14). However, the authors observed a slight decrease in the static strength.

With recent advances in the titanium aluminides, it was observed that under high energy density joining processes (laser and electron beam) the weld zone and the fields above the transition temperature in the heat-affected zone mainly consisted of an unstable β/B2 phase, which significantly deteriorates the high temperature properties of the alloy [113, 212, 213]. Therefore, adjusting the unstable microstructure of the weld zone is necessary. Several studies suggested the use of PWHT to adjust the microstructure and improve the joints performance [128–130, 213]. For example, Wang et al. [213] investigated the effect of the PWHT on the microstructure and mechanical properties of Ti23Al17b laser-welded joints. It was found that the joint tensile ductility significantly improved to 5.50–7.88%, which is higher than that in the as-welded condition when tested at elevated temperature (650 °C) under suitable post weld heat treatment condition (980 °C for 1.5 h, air cooling).

Practically, PWHT of welded structures is challenging and expensive due to high temperature required for effective microstructural change, inert shielding required for preventing interstitial elements ingression, and the loss of strength at elevated temperature. In addition, unless meticulous fixturing is adopted, the distortion is inevitable. Therefore, PWHT is generally used where the property enhancement is a crucial requirement of the design [6, 214].

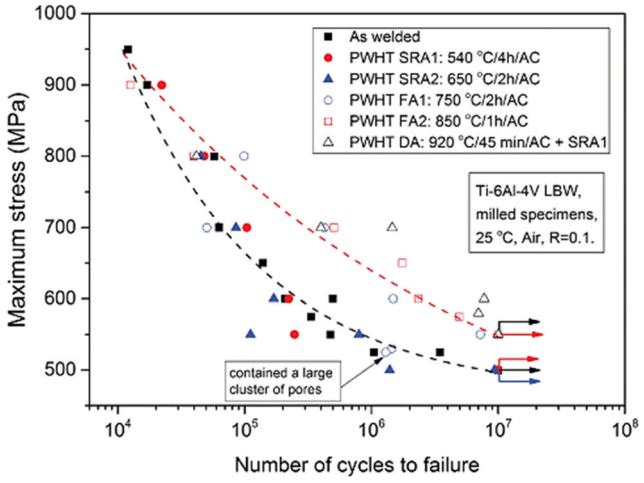

Fig. 14 Effect of PWHT on the fatigue behavior of Ti6Al4V laser weld [33]

8 Main metallurgical defects for titanium alloy laser welds

8.1 Surface oxidation

Titanium is very reactive with ambient elements such as oxygen, nitrogen, hydrogen, and carbon at high temperature. Therefore, the most commonly encountered defects for titanium and its alloys are the formation of hard and brittle titanium oxide surface layer mainly coursed by poor surface preparation, poor cleaning procedures of base metals, and the filler materials before and during welding and/or poor shielding. The formation of the oxide layer can be detected by visual inspection [11, 22–30]. Generally, titanium absorbs hydrogen from 250 °C, oxygen from 400 °C, nitrogen from 600 °C. Several authors observed that the oxygen and nitrogen deteriorate the strength and bending ductility of welds joint; thus, the titanium weld joint embrittlement increases with increasing Ni and O content in the weld [28–30, 215]. Tsay et al. [28] observed that the surface oxidation significantly decreases the tensile ductility of the titanium alloy weld. Therefore, the removal of the hard and brittle surface titanium oxide layer by either mechanical, chemical methods or both before welding is necessary to improve the weld quality [30].

8.2 Micropores

Micropores are formed in the FZ due to the trapped gases within the solidifying weld pool. In titanium welds, several authors suggested that the main mechanism of micropore formation is the hydrogen entering the weld pool which forms pores on solidification [6, 24, 83, 87, 216] and the keyhole instability and collapse at lower welding speeds [11, 28, 64, 217]. Contamination of the weld parts by the presence oil, dirt, etc., is considered as the main sources that supply hydrogen for gas porosity formation [24]. Considerable number of authors suggested for a fully penetrated weld, the micropore

formation is limited [11, 55, 63]. For instance, Hilton et al. [63] laser welded 5-mm-thick Ti6Al4V alloy and reported joints free from pores. The lack of micropores observed was associated with the keyhole formation inside the weld. In comparison, Kumar et al. [11] observed micropores in partially penetrated Ti6Al4V laser-welded sample as shown in Fig. 15a. However, the authors reported that even for a fully penetrated weld, some micropores at the interface of the HAZ and FZ (Fig. 15b) were observed due to keyhole instability and evolution of hydrogen at the solid-liquid interface. Cao et al. [34] laser welded Ti6Al4V alloy with 1- and 2-mm thickness. It was found that for 1-mm-thick joints, the diameter of the micropores was 0.025 mm, whereas, for 2-mm-thick joints, the diameter of the micropores were 0.12 and 0.25 mm. The results of this study suggest that porosity is more likely to appear in thick joints. Furthermore, welding speed has significant influence on the pores formation. Generally, at high welding speed, the solidification is quick and no time for the micropores to grow [60, 83]. For these reasons, titanium alloy thin sheets should be welded under keyhole mode.

Furthermore, a considerable number of studies have reported that the formation of the micropores serves as stress concentrators and greatly reduce the fatigue life of the weld. Therefore, their formation should be minimized to fulfil the strict quality standard [23, 28, 39, 42, 43, 50, 60]. The weld quality acceptance criteria as mentioned in European standard BS EN: 4678 recommended that the size of the micropores should be less than or equal to 0.40 mm [218]. Many works concentrated on finding a solution to prevent micropore formation in titanium alloy welds to improve the weld quality [43, 50, 83, 87, 187, 219, 220]. For instance, Li et al. [50] investigated the stitch laser-welded Ti6Al4V alloys. It was found that the reduction of the laser input power, scanning speed, and positive defocusing distance could significantly suppress the micropores formation in the welded seam, while the existing porosity could be reduced with remelting. Furthermore, Blackburn et al. [43] observed that for titanium alloy welds, the micropore formation depends on the heat input waveform and the modulation of the frequency and amplitude. The authors suggested that the square waveform coupled with higher frequencies effectively minimized the micropores formation compared to continuous wave.

8.3 Microcracks

Titanium alloys are generally resistance to HAZ liquation cracking, because of the absence of second dispersoids or precipitates coupled with limited impurities at grain boundaries. However, the presence of impurities such as iron may cause local melting of the Ti-Fe eutectic called hydrogen delayed cracking [12, 34, 60]. For instance, Ahn et al. [60] laser welded Ti6Al4V alloy using a high power fiber laser. The results indicated that no crack defect was observed. The lack of microcrack observed was associated with the absence of secondary phase dispersoids or precipitate particles, or impurities at the grain boundaries. Similarly, Cao et al. [34] laser welded Ti6Al4V alloy with 1 and 2 mm thickness using high power Nd:YAG laser. The X-ray examination did not reveal any weld cracks for either of the thickness; however, HAZ cracking was occasionally observed. The HAZ microcrack observed was associated with iron capture during primary manufacturing process of the titanium alloy.

8.4 Face/root undercut (underfill)

Face/root underfill/undercut defects have been observed by many researches for laser-welded titanium alloys. The presence of underfill/undercut in the titanium welds serves as stress concentrators and deteriorates the joints properties [23, 34, 39, 60, 64, 73, 84, 98, 122, 221–223]. Generally, the formation of the undercuts defect is related to the high welding speeds, whereas, evaporation of the molten weld metals is considered as the main cause of underfill defects [34, 60, 73, 122, 224]. For instance, Cao et al. [34] reported that the FZ area and the underfill depth depend on the welding speed and suggested welding at higher speed in order to minimize the underfill defects. Ahn et al. [60] laser welded Ti6Al4V alloy. It was observed that high welding power led to spatter and undercut, whereas, incomplete penetration occurred at low laser power and high welding speed. Recently, Kumar et al. [11]

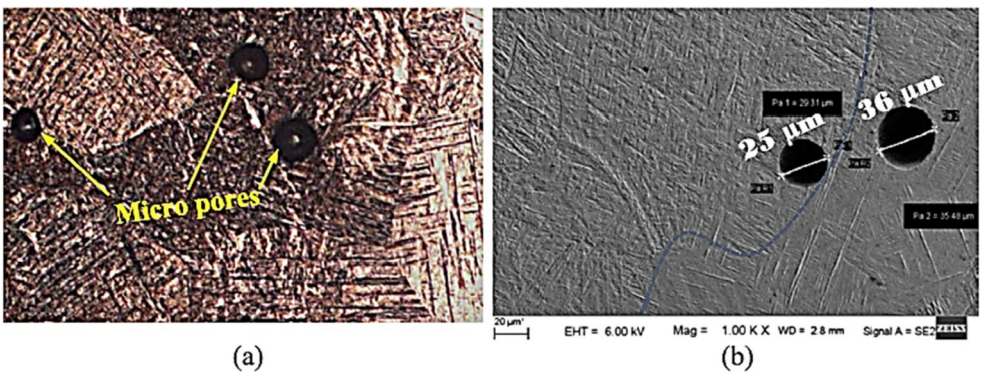

Fig. 15 Typical micropores appearance for a laser-welded Ti6Al4V alloy. **a** Partially melted weld. **b** Solid-liquid interface of a fully penetrated weld [11]

laser welded Ti6Al4V alloy and reported that the underfill and micropores served as stress concentrators for fatigue cracks and significantly degraded the joints mechanical properties. Therefore, their formation should be minimized to fulfil the strict quality standard.

In view of the detrimental effects of underfill on titanium alloys welds, the fusion welding specification for aerospace application (AWS D17.1) recommended that the maximum depth of the underfill for a class A welds should be limited to 7% of the material thickness (7%T) [225]. Therefore, a considerable number of works concentrated on exploring the laser welding techniques to reduce or even suppress the underfill and undercut formation in titanium alloys welds. For instance, using a compatible filler wire has been reported to decrease the number of the underfill/undercut and improve the joint ductility, fatigue life, and tensile strength [82–87]. Kashaev et al. [85] studied Nd:YAG single-sided laser beam welding of Ti-6Al-4V 2.5-mm-thick T-joints with a compatible filler (Titanium Grade 2). The filler wire was found to suppress the underfill and undercut defects. Recently, Fang et al. [108, 226] investigated the effect of transversal pre-extrusion load on underfill formation during laser welding of Ti2Al1.5Mn alloy. It was found that the underfill defects can be minimized or eliminated and high tensile strength can be obtained by welding with pre-extrusion load under suitable laser welding parameters.

9 Future trends

Despite the inherent material properties (such as lightweight, fuel efficiency, and performance) of Ti alloys, the cost of raw material and fabrication overshadowed the wide applications of titanium alloys particularly where the corrosion and weight reduction are not essential factors. Therefore, future research should focus more on the development of more efficient technologies for the manufacture of low-cost complex titanium structures.

Research and development of laser welding techniques for titanium alloys are mainly focused on industrial needs. Therefore, to fully understand the maximum capabilities, further work is needed on modeling and simulation for optimization, controlling, and defining the laser welding parameter-operating windows for different titanium alloys to produce consistently good quality welds.

Interestingly, the use of fiber and disk laser may help to improve the reliability of laser welding techniques in titanium alloys industries because of their low susceptibility to plasma plume formation. Future researchers should therefore focus on using fiber and disk lasers for different grades of titanium alloys.

Welding process imposed microstructural variation of titanium alloys, which affect the corrosion behavior of the welds joints. Because of the corrosion resistance and reliability of weld joints keep a close relation, the investigations of corrosion behavior of laser-welded titanium alloys joints are crucial. However, the studies on the corrosion behaviors of titanium alloys joints are rare.

Titanium alloys are usually applied in fatigue critical components; however, the laser-welded Ti alloys exhibited poor axial fatigue performance. Thus, extensive study on the fatigue life of laser-welded Ti alloys is of great scientific interest.

In order to evaluate the life safety for the critical components and structures, studies on the influence of welding on the fracture toughness is essential. However, few works have been reported on the fracture toughness of titanium alloys under laser beam welding condition.

Another important area that requires a great attention is the control of residual stress distribution and associated deformations due to the welding phenomenon in laser-welded titanium alloys.

Additionally, despite a lot of progress in the laser welding of titanium alloys so far, the effect of post weld heat treatment on the laser-welded Ti alloys joints has not been extensively studied.

Many researchers had reported hybrid structures made from titanium to other metals, but their weldability characteristics and the effect of the transition materials on the dissimilar joints properties have not been clearly understood. Therefore, future researchers should focus on improving joint properties using alternative interlayers.

Dissimilar joints between different titanium and composites will probably gain considerable attention in the future due to the compatibility of titanium alloys with composites and potential applications of titanium-composite hybrid structures in the aerospace industry. However very little work has been done in this aspect.

10 Summary

Recent studies suggested that laser beam welding is a viable option for welding of titanium due its versatility, high specific heat input, and flexibility and facilitates their applications in medical, chemical, aerospace, biomaterial, marine, petrochemical, and aviation industries. The literature reveals that the laser processing parameters have great influence on the joint microstructure and properties. However, titanium alloy laser welds were reported to exhibit some processing problems and weld defects, such as lower elongations, inferior fatigue properties, surface oxidations, porosity, undercut/underfill, and weld cracking. Therefore, scientific observations are needed to better understand and address these problems.

Over the years, varieties of titanium to other metals have been joined by laser beam welding under optimum processing conditions. In particular, Ti/steel, Ti/Al, and Ti/Mg dissimilar alloys have been studies for their mechanical and metallurgical properties. Several authors adopted various techniques to improve the joint strength. These efforts result in the static strength increase of the laser-welded Ti/other metals joints,

but the strength of the dissimilar joints is still low compared to the BM. Therefore, more research efforts are required on the formation mechanism of the IMCs.

References

1. International A, CommitteeAIH, CommitteeAIAPD (1990) Metals handbook: properties and selection, vol 2. Asm International
2. Mordike B, Ebert T (2001) Magnesium: properties—applications—potential. Mater Sci Eng A 302(1):37–45. https://doi.org/10.1016/S0921-5093(00)01351-4
3. FujiiH, TakahashiK, YamashitaY (2003) Application of titanium and its alloys for automobile parts. Shinnittetsu giho:62-67
4. Manladan S, Yusof F, Ramesh S, Fadzil M (2016) A review on resistance spot welding of magnesium alloys. Int J Adv Manuf Technol 86(5-8):1805–1825
5. Baqer YM, Ramesh S, Yusof F, Manladan S (2018) Challenges and advances in laser welding of dissimilar light alloys: Al/Mg, Al/Ti, and Mg/Ti alloys. Int J Adv Manuf Technol 1-17
6. Baeslack W, Becker D, Froes F (1984) Advances in titanium alloy welding metallurgy. JOM 36(5):46–58. https://doi.org/10.1007/BF03338455
7. Shi YW, Zhong F, Li XY, Gong SL, Chen L (2007) Effect of laser beam welding on fracture toughness of a Ti-6.5Al-2Zr-1Mo-1V alloy sheet. J Mater Sci 42(16):6651–6657. https://doi.org/10.1007/s10853-007-1524-y
8. Liu LM, Hao XF, Du X (2008) Microstructure characteristics and mechanical properties of laser-TIG hybrid welding joint of TA15 titanium alloy. Mater Res Innov 12(3):114–118. https://doi.org/10.1179/143307508x333703
9. Lee H-S, Yoon J-H, Yi Y-M (2007) Oxidation behavior of titanium alloy under diffusion bonding. Thermochimica Acta 455(1):105–108. https://doi.org/10.1016/j.tca.2006.12.004
10. Costa A, Miranda R, Quintino L, Yapp D (2007) Analysis of beam material interaction in welding of titanium with fiber lasers. Mater Manuf Process 22(7-8):798–803. https://doi.org/10.1080/10426910701446671
11. Kumar C, Das M, Paul CP, Singh B (2017) Experimental investigation and metallographic characterization of fiber laser beam welding of Ti-6Al-4V alloy using response surface method. Opt Laser Eng 95:52–68. https://doi.org/10.1016/j.optlaseng.2017.03.013
12. Donachie MJ (2000) Titanium: a technical guide. ASM international
13. Gao XL, Zhang LJ, Liu J, Zhang JX (2013) A comparative study of pulsed Nd:YAG laser welding and TIG welding of thin Ti6Al4V titanium alloy plate. Mater Sci Eng A Struct 559:14–21. https://doi.org/10.1016/j.msea.2012.06.016
14. Balasubramanian T, Balasubramanian V, Manickam MM (2011) Fatigue crack growth behaviour of gas tungsten arc, electron beam and laser beam welded Ti–6Al–4V alloy. Mater Design 32(8):4509–4520. https://doi.org/10.1016/j.matdes.2011.03.025
15. Balasubramanian TS, Balasubramanian V, Muthumanikkam MA (2011) Fatigue performance of gas tungsten arc, electron beam, and laser beam welded Ti-6Al-4V alloy joints. J Mater Eng Perform 20(9):1620–1630. https://doi.org/10.1007/s11665-010-9822-y
16. Yunlian Q, Ju D, Quan H, Liying Z (2000) Electron beam welding, laser beam welding and gas tungsten arc welding of titanium sheet. Mater Sci Eng A 280(1):177–181. https://doi.org/10.1016/S0921-5093(99)00662-0
17. Zhang L, Gao X, Sun M, Zhang J (2014) Weld outline comparison between various pulsed Nd: YAG laser welding and pulsed Nd: YAG laser–TIG arc welding. Int J Adv Manuf Technol 75(1-4):153–160. https://doi.org/10.1007/s00170-014-6122-y
18. Zhang JX, Xue Y, Gong SL (2005) Residual welding stresses in laser beam and tungsten inert gas weldments of titanium alloy. Sci Technol Weld Join 10(6):643–646. https://doi.org/10.1179/174329305x48374
19. Kumar C, Das M, Biswas P (2015) A 3-D finite element analysis of transient temperature profile of laser welded Ti-6Al-4V alloy. Lasers Based Manuf:421–440. https://doi.org/10.1007/978-81-322-2352-8_21
20. Auwal ST, Ramesh S, Yusof F, Manladan SM (2018) A review on laser beam welding of copper alloys. Int J Adv Manuf Technol. https://doi.org/10.1007/s00170-017-1566-5
21. Zhan XH, Peng QY, Wei YH, Ou WM (2017) Experimental and simulation study on the microstructure of TA15 titanium alloy laser beam welded joints. Opt Laser Technol 94:279–289. https://doi.org/10.1016/j.optlastec.2017.03.014
22. Caiazzo F, Curcio F, Daurelio G, Minutolo FMC (2004) Ti6Al4V sheets lap and butt joints carried out by CO_2 laser: mechanical and morphological characterization. J Mater Process Technol 149(1):546–552. https://doi.org/10.1016/j.jmatprotec.2003.12.026
23. Akman E, Demir A, Canel T, Sinmazcelik T (2009) Laser welding of Ti6Al4V titanium alloys. J Mater Process Technol 209(8):3705–3713. https://doi.org/10.1016/j.jmatprotec.2008.08.026
24. Chamanfar A, Pasang T, Ventura A, Misiolek WZ (2016) Mechanical properties and microstructure of laser welded Ti-6Al-2Sn-4Zr-2Mo (Ti6242) titanium alloy. Mat Sci Eng A Struct 663:213–224. https://doi.org/10.1016/j.msea.2016.02.068
25. Lisiecki A (2013) Welding of titanium alloy by Disk laser. Laser Technology 2012: Applications of Lasers 8703. Artn 87030t, https://doi.org/10.1117/12.2013431
26. Aleksander APL (2012) Laser welding of titanium alloy Ti6Al4V using a disk laser. MTM J 7:53–56
27. Caiazzo F, Alfieri V, Fierro I, Sergi V (2014) Investigation and optimization of disk-laser welding of 1 mm thick Ti-6al-4v titanium alloy sheets. Proceedings of the Asme 9th International Manufacturing Science and Engineering Conference, 2014, vol 2
28. Tsay L, Shan Y-P, Chao Y-H, Shu W (2006) The influence of porosity on the fatigue crack growth behavior of Ti–6Al–4V laser welds. J Mater Sci 41(22):7498–7505. https://doi.org/10.1007/s10853-006-0833-x
29. Li X, Xie J, Zhou Y (2005) Effects of oxygen contamination in the argon shielding gas in laser welding of commercially pure titanium thin sheet. J Mater Sci 40(13):3437–3443. https://doi.org/10.1007/s10853-005-0447-8
30. Blackburn J, Allen C, Hilton P, Li L (2010) Nd:YAG laser welding of titanium alloys using a directed gas jet. J Laser Appl 22(2):71–78. https://doi.org/10.2351/1.3455825
31. Lei ZL, Dong ZJ, Chen YB, Zhang J, Zhu RC (2013) Microstructure and tensile properties of laser beam welded Ti-22Al-27Nb alloys. Mater Design 46:151–156. https://doi.org/10.1016/j.matdes.2012.10.022
32. Caiazzo F, Alfieri V, Fierro I, Sergi V (2015) Investigation and optimization of disk-Llaser welding of 1 mm thick Ti-6Al-4V titanium alloy sheets. Adv Mech Eng 7(1):Artn 373561. https://doi.org/10.1155/2014/373561
33. Fomin F, Ventzke V, Dorn F, Levichev N, Kashaev N (2017) Effect of microstructure transformations on fatigue properties of laser beam welded Ti-6Al-4V butt joints subjected to postweld heat treatment. In: Study of grain boundary character. InTech

34. Cao X, Jahazi M (2009) Effect of welding speed on butt joint quality of Ti-6Al-4V alloy welded using a high-power Nd:YAG laser. Opt Laser Eng 47(11):1231–1241
35. Zhang Y, Sun DQ, Gu XY, Liu YJ (2017) Nd/YAG pulsed laser welding of TC4 titanium alloy to 301L stainless steel via pure copper interlayer. Int J Adv Manuf Tech 90(1-4):953–961. https://doi.org/10.1007/s00170-016-9453-z
36. Chen Y, Chen S, Li L (2010) Influence of interfacial reaction layer morphologies on crack initiation and propagation in Ti/Al joint by laser welding–brazing. Mater Design 31(1):227–233. https://doi.org/10.1016/j.matdes.2009.06.029
37. Tan CW, Lu QS, Chen B, Song XG, Li LQ, Feng JC, Wang Y (2017) Influence of laser power on microstructure and mechanical properties of laser welded-brazed Mg to Ni coated Ti alloys. Opt Laser Technol 89:156–167. https://doi.org/10.1016/j.optlastec.2016.10.014
38. Amaya-Vazquez M, Sánchez-Amaya J, Boukha Z, Botana F (2012) Microstructure, microhardness and corrosion resistance of remelted TiG2 and Ti6Al4V by a high power diode laser. Corros Sci 56:36–48. https://doi.org/10.1016/j.corsci.2011.11.006
39. Squillace A, Prisco U, Ciliberto S, Astarita A (2012) Effect of welding parameters on morphology and mechanical properties of Ti–6Al–4V laser beam welded butt joints. J Mater Process Technol 212(2):427–436. https://doi.org/10.1016/j.jmatprotec.2011.10.005
40. Tsay L-W, Hsu C-L, Chen C (2010) The influence of microstructures on the notched tensile fracture of Ti–6Al–6V–2Sn welds at elevated temperatures. Isij Int 50(1):128–132. https://doi.org/10.2355/isijinternational.50.128
41. Wang S, Wei M, Tsay L (2003) Tensile properties of LBW welds in Ti–6Al–4V alloy at evaluated temperatures below 450 C. Mater Lett 57(12):1815–1823
42. Nakai M, Niinomi M, Akahori T, Hayashi K, Itsumi Y, Murakami S, Oyama H, Abe W (2012) Microstructural factors determining mechanical properties of laser-welded Ti-4.5Al-2.5Cr-1.2Fe-0.1C alloy for use in next-generation aircraft. Mat Sci Eng A Struct 550:55–65. https://doi.org/10.1016/j.msea.2012.04.022
43. Blackburn J, Allen C, Hilton P, Li L, Hoque M, Khan A (2010) Modulated Nd: YAG laser welding of Ti–6Al–4V. Sci Technol Weld Join 15(5):433–439. https://doi.org/10.1179/136217110X12731414739718
44. Gao X-L, Zhang L-J, Liu J, Zhang J-X (2014) Porosity and microstructure in pulsed Nd: YAG laser welded Ti6Al4V sheet. J Mater Process Technol 214(7):1316–1325. https://doi.org/10.1016/j.jmatprotec.2014.01.015
45. Balasubramanian T, Balakrishnan M, Balasubramanian V, Manickam MM (2011) Influence of welding processes on microstructure, tensile and impact properties of Ti-6Al-4V alloy joints. Trans Nonferrous Metals Soc China 21(6):1253–1262. https://doi.org/10.1016/S1003-6326(11)60850-9
46. Lisiecki A (2012) Welding of titanium alloy by different types of lasers. Arch Mater Sci Eng 58(2):209–218
47. Caiazzo F, Cardaropoli F, Alfieri V, Sergi V, Argenio P, Barbieri G (2017) Disk-laser welding of Ti-6Al-4V titanium alloy plates in T-joint configuration.17th International Conference on Sheet Metal (Shemet17) 183:219-226. https://doi.org/10.1016/j.proeng.2017.04.024
48. Liu H, Nakata K, Yamamoto N, Liao J (2011) Mechanical properties and strengthening mechanisms in laser beam welds of pure titanium. Sci Technol Weld Join 16(7):581–585. https://doi.org/10.1179/1362171811Y.0000000054
49. Liu H, Nakata K, Yamamoto N, Liao J (2012) Microstructural characteristics and mechanical properties in laser beam welds of Ti6Al4V alloy. J Mater Sci 47(3):1460–1470. https://doi.org/10.1007/s10853-011-5931-8
50. Li C, Li B, Wu ZF, Qi XY, Ye B, Wang AH (2017) Stitch welding of Ti-6Al-4V titanium alloy by fiber laser. Trans Nonferrous Metals Soc China 27(1):91–101. https://doi.org/10.1016/S1003-6326(17)60010-4
51. Evtihiev NN, Grezev NV, Markushov YV, Murzakov MA (2016) Fiber lasers application for welding of titanium alloys with 16 mm thickness. Ii Conference on Plasma & Laser Research and Technologies 747. Unsp 012061, https://doi.org/10.1088/1742-6596/747/1/012061
52. Campanelli SL, Casalino G, Mortello M, Angelastro A, Ludovico AD (2015) Microstructural characteristics and mechanical properties of Ti6Al4V alloy fiber laser welds. Procedia CIRP 33:428–433
53. Cao X, Jahazi M, Immarigeon J, Wallace W (2006) A review of laser welding techniques for magnesium alloys. J Mater Process Technol 171(2):188–204
54. Mueller S, Bratt C, Mueller P, Cuddy J, Shankar K (2008) Laser beam welding of titanium—a comparison of CO_2 and fiber laser for potential aerospace applications. In: Proceedings of ICALEO 2008: 27th International Congress on Applications of Lasers and Electro-Optics, pp 846-854
55. Caiazzo F, Alfieri V, Corrado G, Cardaropoli F, Sergi V (2013) Investigation and optimization of laser welding of Ti-6Al-4 V titanium alloy plates. J Manuf Sci E-T ASME 135(6):Unsp 061012. https://doi.org/10.1115/1.4025578
56. Giesen A, Speiser J (2007) Fifteen years of work on thin-disk lasers: results and scaling laws. IEEE J Select Top Quantum Electron 13(3):598–609
57. Bharti A (1988) Laser welding. Bull Mater Sci 11(2):191–212. https://doi.org/10.1007/BF02744554
58. Zhao Y, Huang J, Zhao Y, Wu YX (2011) Microstructure and mechanical properties of laser welded lap joints of Ti-6Al-4V alloy. Adv Mater Process Pts 1-3 311-313:2375-2378. https://doi.org/10.4028/www.scientific.net/AMR.311-313.2375
59. Sun Z, Pan D, Zhang W (2002) Correlation between welding parameters and microstructures in TIG, plasma and laser welded Ti-6 Al-4 V alloy. In: 6th International Conference: trends in welding research, pp 760-767
60. Ahn J, Chen L, Davies C, Dear J (2016) Parametric optimisation and microstructural analysis on high power Yb-fibre laser welding of Ti–6Al–4V. Opt Laser Eng 86:156–171. https://doi.org/10.1016/j.optlaseng.2016.06.002
61. Liu J, Watanabe I, Yoshida K, Atsuta M (2002) Joint strength of laser-welded titanium. Dent Mater 18(2):143–148. https://doi.org/10.1016/S0109-5641(01)00033-1
62. Junaid M, Khan FN, Rahman K, Baig MN (2017) Effect of laser welding process on the microstructure, mechanical properties and residual stresses in Ti-5Al-2.5 Sn alloy. Opt Laser Technol
63. Hilton P, Blackburn J, Chong P (2007) Welding of Ti-6Al-4V with fibre delivered laser beams. In: Proceedings of ICALEO, pp 887-895
64. Kabir ASH, Cao X, Gholipour J, Wanjara P, Cuddy J, Birur A, Medraj M (2012) Effect of postweld heat treatment on microstructure, hardness, and tensile properties of laser-welded Ti-6Al-4V. Metall Mater Trans A 43(11):4171–4184. https://doi.org/10.1007/s11661-012-1230-5
65. Buddery A, Kelly P, Drennan J, Dargusch M (2011) The effect of contamination on the metallurgy of commercially pure titanium welded with a pulsed laser beam. J Mater Sci 46(8):2726–2732. https://doi.org/10.1007/s10853-010-5145-5
66. Lee H-K, Han H-S, Son K-J, Hong S-B (2006) Optimization of Nd: YAG laser welding parameters for sealing small titanium tube ends. Mater Sci Eng A 415(1):149–155. https://doi.org/10.1016/j.msea.2005.09.059
67. Tzeng Y-F (2000) Process characterisation of pulsed Nd: YAG laser seam welding. Int J Adv Manuf Technol 16(1):10–18. https://doi.org/10.1007/PL00013126

68. Blackburn JE, Allen CM, Hilton PA, Li L (2010) Dual focus Nd: YAG laser welding of titanium alloys. Proceedings of the 36th International Matador Conference, pp 279-282. https://doi.org/10.1007/978-1-84996-432-6_64
69. Torkamany M, Hamedi M, Malek F, Sabbaghzadeh J (2006) The effect of process parameters on keyhole welding with a 400 W Nd: YAG pulsed laser. J Phys D Appl Phys 39(21):4563. https://doi.org/10.1088/0022-3727/39/21/009
70. Fang X, Liu H, Zhang J (2014) Microstructure and mechanical properties of pulsed laser beam welded Ti-2Al-1.5 Mn titanium alloy joints. J Mater Eng Perform 23(6):1973–1980
71. Chen SH, Huang JH, Cheng DH, Zhang H, Zhao XK (2012) Superplastic deformation mechanism and mechanical behavior of a laser-welded Ti-6Al-4V alloy joint. Mat Sci Eng A Struct 541:110–119. https://doi.org/10.1016/j.msea.2012.02.011
72. Cheng DH, Huang JH, Zhao XK, Zhang H (2010) Microstructure and superplasticity of laser welded Ti-6Al-4V alloy. Mater Des 31(1):620–623. https://doi.org/10.1016/j.matdes.2009.06.020
73. Fang XY, Zhang JX (2015) Effects of microstructure and concavity on damage behavior of laser beam welded Ti-2Al-1.5Mn titanium alloy joints. Int J Adv Manuf Technol 79(9-12):1557–1568. https://doi.org/10.1007/s00170-015-6924-6
74. Fang XY, Liu H, Zhang JX (2014) Microstructure and mechanical properties of pulsed laser beam welded Ti-2Al-1.5Mn titanium alloy joints. J Mater Eng Perform 23(6):1973–1980. https://doi.org/10.1007/s11665-014-1002-z
75. Shinoda T, Matsunaga K, Shinhara M (1991) Laser welding of titanium alloy. Weld Int 5(5):346–351. https://doi.org/10.1080/09507119109446749
76. Schneider A, Gumenyuk A, Lammers M, Malletschek A, Rethmeier M (2014) Laser beam welding of thick titanium sheets in the field of marine technology.8th International Conference on Laser Assisted Net Shape Engineering (Lane 2014) 56:582-590. https://doi.org/10.1016/j.phpro.2014.08.046
77. Denney P, Metzbower E (1989) Laser beam welding of titanium. Weld J 68(8):342s–346s
78. Guo W, Li RT, Zhu Y, Liu Q, Qu P, Kang H (2013) Superplastic tensile behavior and microstructure evolution of laser welded Ti-6Al-4V alloy. Rare Metal Mater Eng 42:74–77
79. Liu H, Nakata K, Zhang J, Yamamoto N, Liao J (2012) Microstructural evolution of fusion zone in laser beam welds of pure titanium. Mater Charact 65:1–7. https://doi.org/10.1016/j.matchar.2011.12.010
80. Casalino G, Curcio F, Minutolo FMC (2005) Investigation on Ti6Al4V laser welding using statistical and Taguchi approaches. J Mater Process Technol 167(2):422–428. https://doi.org/10.1016/j.jmatprotec.2005.05.031
81. Ahn J, He E, Chen L, Dear J, Davies C (2017) The effect of Ar and He shielding gas on fibre laser weld shape and microstructure in AA 2024-T3. J Manuf Process 29:62–73. https://doi.org/10.1016/j.jmapro.2017.07.011
82. Cao XJ, Debaecker G, Jahazi M, Marya S, Cuddy J, Birur A Effect of post-weld heat treatment on Nd: YAG laser welded Ti-6Al-4V alloy quality. In: Materials Science Forum, 2010. Trans Tech Publ, pp 3655-3660. https://doi.org/10.4028/www.scientific.net/MSF.638-642.3655
83. Khaled Z (1994) An investigation of pore cracking in titanium welds. J Mater Eng Perform 3(3):419–434. https://doi.org/10.1007/BF02645341
84. Shariff T, Cao X, Chromik RR, Wanjara P, Cuddy J, Birur A (2012) Effect of joint gap on the quality of laser beam welded near-beta Ti-5553 alloy with the addition of Ti-6Al-4V filler wire. J Mater Sci 47(2):866–875. https://doi.org/10.1007/s10853-011-5866-0
85. Kashaev N, Ventzke V, Fomichev V, Fomin F, Riekehr S (2016) Effect of Nd: YAG laser beam welding on weld morphology and mechanical properties of Ti–6Al–4V butt joints and T-joints. Opt Laser Eng 86:172–180. https://doi.org/10.1016/j.optlaseng.2016.06.004
86. Abbasi K, Beidokhti B, Sajjadi S (2017) Microstructure and mechanical properties of Ti-6Al-4V welds using α, near-α and α+ β filler alloys. Mater Sci Eng A. https://doi.org/10.1016/j.msea.2017.07.027
87. Cao X, Debaecker G, Poirier E, Marya S, Cuddy J, Birur A, Wanjara P (2011) Tolerances of joint gaps in Nd:YAG laser welded Ti-6Al-4V alloy with the addition of filler wire. J Laser Appl 23(1):Artn 012004. https://doi.org/10.2351/1.3554266
88. Dilthey U, Fuest D, Scheller W (1995) Laser welding with filler wire. Opt Quant Electron 27(12):1181–1191. https://doi.org/10.1007/BF00326474
89. Tan C, Chen B, Meng S, Zhang K, Song X, Zhou L, Feng J (2016) Microstructure and mechanical properties of laser welded-brazed Mg/Ti joints with AZ91 Mg based filler. Mater Design 99:127–134
90. Tan C, Song X, Chen B, Li L, Feng J (2016) Enhanced interfacial reaction and mechanical properties of laser welded-brazed Mg/Ti joints with Al element from filler. Mater Lett 167:38–42
91. Cai X, Sun D, Li H, Guo H, Gu X, Zhao Z (2017) Microstructure characteristics and mechanical properties of laser-welded joint of γ-TiAl alloy with pure Ti filler metal. Opt Laser Technol 97:242–247. https://doi.org/10.1016/j.optlastec.2017.07.011
92. Kumar A, Gupta MC (2009) Surface preparation of Ti-3Al-2.5 V alloy tubes for welding using a fiber laser. Opt Laser Eng 47(11):1259–1265. https://doi.org/10.1016/j.optlaseng.2009.05.011
93. Bertrand C, Laplanche O, Rocca J, Le Petitcorps Y, Nammour S (2007) Effect of the combination of different welding parameters on melting characteristics of grade 1 titanium with a pulsed Nd–Yag laser. Laser Med Sci 22(4):237–244. https://doi.org/10.1007/s10103-006-0438-2
94. Kumar A, Sapp M, Vincelli J, Gupta MC (2010) A study on laser cleaning and pulsed gas tungsten arc welding of Ti-3Al-2.5V alloy tubes. J Mater Process Technol 210(1):64–71. https://doi.org/10.1016/j.jmatprotec.2009.08.017
95. Turner M, Schmidt M, Li L (2005) Preliminary study into the effects of YAG laser processing of titanium 6Al–4V alloy for potential aerospace component cleaning application. Appl Surf Sci 247(1):623–630. https://doi.org/10.1016/j.apsusc.2005.01.097
96. Turner M, Crouse P, Li L (2006) Comparison of mechanisms and effects of Nd: YAG and CO 2 laser cleaning of titanium alloys. Appl Surf Sci 252(13):4792–4797. https://doi.org/10.1016/j.apsusc.2005.06.050
97. Li H, Costil S, Liao H, Coddet C, Barnier V, Oltra R (2008) Surface preparation by using laser cleaning in thermal spray. J Laser Appl 20(1):12–21. https://doi.org/10.2351/1.2831623
98. Gao X-L, Zhang L-J, Liu J, Zhang J-X (2014) Effects of weld cross-section profiles and microstructure on properties of pulsed Nd: YAG laser welding of Ti6Al4V sheet. Int J Adv Manuf Technol 72(5-8):895–903. https://doi.org/10.1007/s00170-014-5722-x
99. Gang T, Shi DH, Yuan Y, Yang SY (2006) Segmentation of small defects in laser weld of titanium alloy with complex structure. Insight 48(12):731–734. https://doi.org/10.1784/insi.2006.48.12.731
100. Wang M, Jiang ML, Wei Q, Gu KF (2011) Technique of laser-TIG hybrid T-shape joint welding of titanium alloy. Mater Process Technol Pts 1-4 291-294:841–847. https://doi.org/10.4028/www.scientific.net/AMR.291-294.841
101. Sun Z, Ion J (1995) Laser welding of dissimilar metal combinations. J Mater Sci 30(17):4205–4214. https://doi.org/10.1007/BF00361499
102. Cheng DH, Huang JH, Chen YP, Hu DA (2012) Microstructure evolution characterization of weld joints by laser welding for superplastic deformation of titanium alloy. Rare Metal Mat Eng 41(2):368–371

103. Cao X, Debaecker G, Poirier E, Marya S, Cuddy J, Birur A, Wanjara P (2009) Effect of joint gap on Nd: YAG laser welded Ti-6Al-4V. In: ICALEO 2009 Conference Proceedings, pp 1614-1623
104. Junaid M, Baig MN, Shamir M, Khan FN, Rehman K, Haider J (2017) A comparative study of pulsed laser and pulsed TIG welding of Ti-5Al-2.5Sn titanium alloy sheet. J Mater Process Technol 242: 24–38. https://doi.org/10.1016/j.jmatprotec.2016.11.018
105. Sun Z, Annergren I, Pan D, Mai T (2003) Effect of laser surface remelting on the corrosion behavior of commercially pure titanium sheet. Mater Sci Eng A 345(1):293–300. https://doi.org/10.1016/S0921-5093(02)00477-X
106. Zhang JB, Fan D, Sun YN, Zheng YF (2007) Microstructure and hardness of the laser surface Treated titanium. In: Key Engineering Materials. Trans Tech Publ, pp 1745-1748. https://doi.org/10.4028/www.scientific.net/KEM.353-358.1745
107. Zhang M, Yang D, Chen G (2014) Study on microstructure and properties of laser-MIG hybrid welding joints for Ti-70 alloy. Mach Des Manuf Eng Iii:128–132. https://doi.org/10.4028/www.scientific.net/AMM.607.128
108. Fang XY, Liu H, Zhang JX (2015) Reducing the underfill rate of pulsed laser welding of titanium alloy through the application of a transversal pre-extrusion load. J Mater Process Technol 220:124–134. https://doi.org/10.1016/j.jmatprotec.2015.01.015
109. Dey S, Roy S, Suwas S, Fundenberger J, Ray R (2010) Annealing response of the intermetallic alloy Ti–22Al–25Nb. Intermetallics 18(6):1122–1131. https://doi.org/10.1016/j.intermet.2010.02.010
110. Lei ZL, Dong ZJ, Chen YB, Huang L, Zhu RC (2013) Microstructure and mechanical properties of laser welded Ti-22Al-27Nb/TC4 dissimilar alloys. Mat Sci Eng A Struct 559: 909–916. https://doi.org/10.1016/j.msea.2012.09.057
111. Zhang KZ, Liu M, Lei ZL, Chen YB (2014) Microstructure evolution and tensile properties of laser-TIG hybrid welds of Ti2AlNb-based titanium aluminide. J Mater Eng Perform 23(10): 3778–3785. https://doi.org/10.1007/s11665-014-1153-y
112. Boehlert C, Majumdar B, Seetharaman V, Miracle D (1999) Part I. The microstructural evolution in Ti-Al-Nb O+ BCC orthorhombic alloys. Metall Mater Trans A 30(9):2305–2323. https://doi.org/10.1007/s11661-999-0240-4
113. Wu A, Zou G, Ren J, Zhang H, Wang G, Liu X, Xie M (2002) Microstructures and mechanical properties of Ti–24Al–17Nb (at.%) laser beam welding joints. Intermetallics 10(7):647–652. https://doi.org/10.1016/S0966-9795(02)00049-3
114. Bendersky L, Roytburd A, Boettinger W (1994) Phase transformations in the (Ti, Al) 3 Nb section of the Ti– Al– Nb system—I. Microstructural predictions based on a subgroup relation between phases. Acta Metall Mater 42(7):2323–2335. https://doi.org/10.1016/0956-7151(94)90311-5
115. Kong BB, Liu G, Wang DJ, Wang KH, Yuan SJ (2016) Microstructural investigations for laser welded joints of Ti-22Al-25Nb alloy sheets upon large deformation at elevated temperature. Mater Design 90:723–732. https://doi.org/10.1016/j.matdes.2015.11.007
116. Chen YB, Zhang KZ, Hu X, Lei ZL, Ni LC (2016) Study on laser welding of a Ti-22Al-25Nb alloy: microstructural evolution and high temperature brittle behavior. J Alloy Compd 681:175–185
117. Raghavan V (2005) Al-Nb-Ti (aluminum-niobium-titanium). J Phase Equilib Diffus 26(4):360–368. https://doi.org/10.1361/154770305X56827
118. Mao JW, Lu WJ, Wang LQ, Qin JN, Zhang D (2014) Microstructures and mechanical properties in laser beam welds of titanium matrix composites. Sci Technol Weld Joi 19(2):142–149. https://doi.org/10.1179/1362171813y.0000000176
119. Wang KH, Liu G, Yuan SJ (2015) Deformation behaviour of laser-welded tube blank of TA15 Ti-alloy for gas forming at elevated temperature.4th International Conference on New Forming Technology (Icnft 2015) 21. ARTN 06005. https://doi.org/10.1051/matecconf/20152106005
120. Ahmed T, Rack H (1998) Phase transformations during cooling in α+ β titanium alloys. Mater Sci Eng A 243(1):206–211. https://doi.org/10.1016/S0921-5093(97)00802-2
121. Sarre B, Flouriot S, Geandier G, Panicaud B, de Rancourt V (2016) Mechanical behavior and fracture mechanisms of titanium alloy welded joints made by pulsed laser beam welding. Procedia Struct Int 2:3569–3576. https://doi.org/10.1016/j.prostr.2016.06.445
122. Cao X, Kabir ASH, Wanjara P, Gholipour J, Birur A, Cuddy J, Medraj M (2014) Global and local mechanical properties of autogenously laser welded Ti-6Al-4V. Metall Mater Trans A 45(3): 1258–1272. https://doi.org/10.1007/s11661-013-2106-z
123. Lutjering G (1998) Influence of processing on microstructure and mechanical properties of (alpha+beta) titanium alloys. Mat Sci Eng A Struct 243(1-2):32–45. https://doi.org/10.1016/S0921-5093(97)00778-8
124. Yang CL, Lin SB, Zhang QT (2003) Effect of YF3 on weld microstructure and performance of titanium alloy TC4 in TIG welding. T Nonferr Metal Soc 13:18–21
125. Lee WV, Nicholls JI, Butson TJ, Daly CH (1997) Fatigue life of a Nd: YAG laser-welded metal ceramic alloy. Int J Prosthodont 10(5)
126. Wu YL, Xin HT, Zhang CB, Tang ZB, Zhang ZY, Wang WF (2014) Mechanical properties of thin films of laser-welded titanium and their associated welding defects. Laser Med Sci 29(6): 1799–1805. https://doi.org/10.1007/s10103-013-1334-1
127. Tsay LW, Hsu C (2009) Notched tensile fracture of Ti-6Al-6V-2Sn welds at elevated temperature. In: Advanced Materials Research. Trans Tech Publ, pp 1137-1140. https://doi.org/10.4028/www.scientific.net/AMR.79-82.1137
128. Liu J, Staron P, Riekehr S, Stark A, Schell N, Huber N, Schreyer A, Müller M, Kashaev N (2016) Phase transformation and residual stress in a laser beam spot-welded TiAl-based alloy. Metall Mater Trans A 47(12):5750–5760. https://doi.org/10.1007/s11661-016-3745-7
129. Liu J, Dahmen M, Ventzke V, Kashaev N, Poprawe R (2013) The effect of heat treatment on crack control and grain refinement in laser beam welded β-solidifying TiAl-based alloy. Intermetallics 40:65–70. https://doi.org/10.1016/j.intermet.2013.04.007
130. Liu J, Ventzke V, Staron P, Schell N, Kashaev N, Huber N (2012) Investigation of in situ and conventional post-weld heat treatments on dual-laser-beam-welded γ-TiAl-based alloy. Adv Eng Mater 14(10):923–927. https://doi.org/10.1002/adem.201200113
131. Dunford D, Wisbey A, Partridge P (1991) Effect of superplastic deformation on microstructure, texture, and tensile properties of Ti–6AI–4V. Mater Sci Tech-Lond 7(1):62–70
132. Cheng D, Huang J, Zhang H, Zhao X (2010) Superplastic deformation of laser welded Ti–6Al–4V sheet. Mater Sci Tech-Lond 26(4):457–460
133. Cheng DH, Huang JH, Yang J, Zhang H, Guo HP (2010) Superplastic deformation mechanical behavior of laser welded joints of TC4 titanium alloys. Rare Metal Mater Eng 39(2):277–280
134. Wang KH, Liu G, Tao W, Zhao J, Huang K (2017) Study on the mixed dynamic recrystallization mechanism during the globularization process of laser-welded TA15 Ti-alloy joint under hot tensile deformation. Mater Charact 126:57–63
135. Gang W, Zhang W-C, Zhang G-L, Xu Z-L (2009) Superplastic formability of Ti-6Al-4V butt-welded plate by laser beam welding. T Nonferr Metal Soc 19:s429–s433
136. Kashaev N, Ventzke V, Horstmann M, Riekehr S, Yashin G, Stutz L, Beck W (2015) Microstructure and mechanical properties of laser beam welded joints between fine-grained and standard Ti-6Al-4V sheets subjected to superplastic forming. Adv Eng Mater 17(3):374–382

137. Wu G, Shi C, Sha W, Sha A, Jiang H (2013) Effect of microstructure on the fatigue properties of Ti–6Al–4V titanium alloys. Mater Des 46:668–674. https://doi.org/10.1016/j.matdes.2012.10.059
138. Casavola C, Pappalettere C, Tattoli F (2009) Experimental and numerical study of static and fatigue properties of titanium alloy welded joints. Mech Mater 41(3):231–243. https://doi.org/10.1016/j.mechmat.2008.10.015
139. Amaya-Vázquez M, Sánchez-Amaya J, Boukha Z, El Amrani K, Botana FJ (2012) Application of laser remelting treatments to improve the properties of Ti6Al4V alloy. In: Materials Science Forum. Trans Tech Publ, pp 25-30. https://doi.org/10.4028/www.scientific.net/MSF.713.25
140. Yue T, Yu J, Mei Z, Man H (2002) Excimer laser surface treatment of Ti–6Al–4V alloy for corrosion resistance enhancement. Mater Lett 52(3):206–212. https://doi.org/10.1016/S0167-577X(01)00395-0
141. Zaveri N, Mahapatra M, Deceuster A, Peng Y, Li L, Zhou A (2008) Corrosion resistance of pulsed laser-treated Ti–6Al–4V implant in simulated biofluids. Electrochimica Acta 53(15):5022–5032. https://doi.org/10.1016/j.electacta.2008.01.086
142. Badekas H, Panagopoulos C, Economou S (1994) Laser surface-treatment of titanium. J Mater Process Technol 44(1-2):54–60. https://doi.org/10.1016/0924-0136(94)90037-X
143. Garcia I, De Damborenea J (1998) Corrosion properties of TiN prepared by laser gas alloying of Ti and Ti6Al4V. Corros Sci 40(8):1411–1419. https://doi.org/10.1016/S0010-938X(98)00046-8
144. Yue T, Cheung T, Man H (2000) The effects of laser surface treatment on the corrosion properties of Ti-6Al-4V alloy in Hank's solution. J Mater Sci Lett 19(3):205–208. https://doi.org/10.1023/A:1006750422831
145. Zhu YP, Li CY, Zhang LY (2014) Effects of cryo-treatment on corrosion behavior and mechanical properties of laser-welded commercial pure titanium. Mater Trans 55(3):511–516. https://doi.org/10.2320/matertrans.M2013373
146. Manladan S, Yusof F, Ramesh S, Fadzil M, Luo Z, Ao S (2017) A review on resistance spot welding of aluminum alloys. Int J Adv Manuf Technol 90(1-4):605–634. https://doi.org/10.1007/s00170-016-9225-9
147. Hagiwara M, Emura S, Araoka A, Kong B-O, Tang F (2003) Enhanced mechanical properties of orthorhombic Ti2AlNb-based intermetallic alloy. Met Mater Int 9(3):265–272. https://doi.org/10.1007/BF03027045
148. Boehlert C, Cowen C, Jaeger C, Niinomi M, Akahori T (2005) Tensile and fatigue evaluation of Ti–15Al–33Nb (at.%) and Ti–21Al–29Nb (at.%) alloys for biomedical applications. Mater Sci Eng C 25(3):263–275. https://doi.org/10.1016/j.msec.2004.12.011
149. Çam G, Koçak M (1998) Progress in joining of advanced materials. Int Mater Rev 43(1):1–44. https://doi.org/10.1179/imr.1998.43.1.1
150. Li DL, Hu SS, Shen JQ, Zhang H, Bu XZ (2016) Microstructure and mechanical properties of laser-welded joints of Ti-22Al-25Nb/TA15 dissimilar titanium alloys. J Mater Eng Perform 25(5):1880–1888. https://doi.org/10.1007/s11665-016-2025-4
151. Threadgill P (1995) The prospects for joining titanium aluminides. Mater Sci Eng A 192:640–646. https://doi.org/10.1016/0921-5093(94)03346-3
152. Shen JQ, Li B, Hu SS, Zhang H, Bu XZ (2017) Comparison of single-beam and dual-beam laser welding of Ti-22A1-25Nb/TA15 dissimilar titanium alloys. Opt Laser Technol 93:118–126. https://doi.org/10.1016/j.optlastec.2017.02.013
153. Zhang H, Hu SS, Shen JQ, Li DL, Bu XZ (2015) Effect of laser beam offset on microstructure and mechanical properties of pulsed laser welded BTi-6431S/TA15 dissimilar titanium alloys. Opt Laser Technol 74:158–166. https://doi.org/10.1016/j.optlastec.2015.06.006
154. Zhang K, Lei Z, Chen Y, Liu M, Liu Y (2015) Microstructure characteristics and mechanical properties of laser-TIG hybrid welded dissimilar joints of Ti–22Al–27Nb and TA15. Opt Laser Technol 73:139–145. https://doi.org/10.1016/j.optlastec.2015.04.028
155. Ghosh M, Chatterjee S (2002) Characterization of transition joints of commercially pure titanium to 304 stainless steel. Mater Charact 48(5):393–399. https://doi.org/10.1016/S1044-5803(02)00306-6
156. Hiraga H, Fukatsu K, Ogawa K, Nakayama M, Muto Y (2002) Nd: YAG laser welding of pure titanium to stainless steel. Weld Int 16(8):623–631. https://doi.org/10.1080/09507110209549587
157. Murray JL (1987) Phase diagrams of binary titanium alloys. ASM Int 1987:354
158. Xian A-P, Si Z-Y (1992) Interlayer design for joining pressureless sintered sialon ceramic and 40Cr steel brazing with Ag 57 Cu 38 Ti 5 filler metal. J Mater Sci 27(6):1560–1566
159. Tomashchuk I, Sallamand P, Andrzejewski H, Grevey D (2011) The formation of intermetallics in dissimilar Ti6Al4V/copper/AISI 316 L electron beam and Nd: YAG laser joints. Intermetallics 19(10):1466–1473. https://doi.org/10.1016/j.intermet.2011.05.016
160. Gao Y, Tsumura T, Nakata K (2012) Dissimilar welding of titanium alloys to steels
161. Zhao S, Yu G, He X, Zhang Y, Ning W (2011) Numerical simulation and experimental investigation of laser overlap welding of Ti6Al4V and 42CrMo. J Mater Process Technol 211(3):530–537. https://doi.org/10.1016/j.jmatprotec.2010.11.007
162. Chen SH, Zhang MX, Huang JH, Cui CJ, Zhang H, Zhao XK (2014) Microstructures and mechanical property of laser butt welding of titanium alloy to stainless steel. Mater Des 53:504–511. https://doi.org/10.1016/j.matdes.2013.07.044
163. Mohid Z, Liman MA, Rahman MRA, Rafai NH, Rahim EA (2014) Dissimilar materials laser welding characteristics of stainless steel and titanium alloy. Appl Mech Mater 465-466:1060–1064. https://doi.org/10.4028/www.scientific.net/AMM.465-466.1060
164. Cherepanov A, Orishich A, Mali V (2014) Laser welding of stainless steel with a titanium alloy with the use of a multilayer insert obtained in an explosion. Combustion Explosion Shock Waves 50(4):483–487. https://doi.org/10.1134/S0010508214040182
165. Shanmugarajan B, Padmanabham G (2012) Fusion welding studies using laser on Ti–SS dissimilar combination. Opt Laser Eng 50(11):1621–1627. https://doi.org/10.1016/j.optlaseng.2012.05.008
166. Satoh G, Yao YL, Qiu C (2013) Strength and microstructure of laser fusion-welded Ti–SS dissimilar material pair. Int J Adv Manuf Technol 66(1):469–479. https://doi.org/10.1007/s00170-012-4342-6
167. Kireev L, Zamkov V (2002) Fusion welding of titanium to steel. Paton Weld J C/C Avtomaticheskaia Svarka 2002(8):28–29
168. Tomashchuk I, Sallamand P, Belyavina N, Pilloz M (2013) Evolution of microstructures and mechanical properties during dissimilar electron beam welding of titanium alloy to stainless steel via copper interlayer. Mat Sci Eng A Struct 585:114–122. https://doi.org/10.1016/j.msea.2013.07.050
169. Tomashchuk I, Sallamand P, Jouvard J (2011) Multiphysical modeling of dissimilar welding via interlayer. J Mater Process Technol 211(11):1796–1803. https://doi.org/10.1016/j.jmatprotec.2011.06.004
170. Tomashchuk I, Grevey D, Sallamand P (2015) Dissimilar laser welding of AISI 316L stainless steel to Ti6-Al4-6V alloy via pure vanadium interlayer. Mat Sci Eng A Struct 622:37–45. https://doi.org/10.1016/j.msea.2014.10.084
171. Zhang Y, Sun DQ, Gu XY, Li HM (2016) A hybrid joint based on two kinds of bonding mechanisms for titanium alloy and stainless steel by pulsed laser welding. Mater Lett 185:152–155. https://doi.org/10.1016/j.matlet.2016.08.138

172. Mitelea I, Groza C, Craciunescu C (2013) Copper interlayer contribution on Nd:YAG laser welding of dissimilar Ti-6Al-4V alloy with X5CrNi18-10 steel. J Mater Eng Perform 22(8):2219–2223. https://doi.org/10.1007/s11665-013-0507-1
173. Li HM, Sun DQ, Gu XY, Dong P, Lv ZP (2013) Effects of the thickness of Cu filler metal on the microstructure and properties of laser-welded TiNi alloy and stainless steel joint. Mater Des 50: 342–350. https://doi.org/10.1016/j.matdes.2013.03.014
174. Groza C, Mitelea I, Uțu I, Crăciunescu CM (2012) Melted zone morphology by laser welding of Ti-6Al-4V with X5CrNi18-10. In: 21nd International Conference on Metallurgy and Materials. Brno, Czech Republic, p 113
175. Pugacheva NB, Myasnikova MV, Michurov NS (2016) Simulation of the elastic deformation of laser-welded joints of an austenitic corrosion-resistant steel and a titanium alloy with an intermediate copper insert. Phys Met Metallogr+ 117(2): 195–203. https://doi.org/10.1134/S0031918x15120078
176. Okamoto H (2002) Cu-Ti (copper-titanium). J Phase Equilib 23(6):549–550. https://doi.org/10.1361/105497102770331307
177. Gao M, Chen C, Wang L, Wang ZM, Zeng XY (2015) Laser-arc hybrid welding of dissimilar titanium alloy and stainless steel using copper wire. Metall Mater Trans A 46A(5):2007–2020. https://doi.org/10.1007/s11661-015-2798-3
178. DebRoy T, Bhadeshia H (2010) Friction stir welding of dissimilar alloys—a perspective. Sci Technol Weld Join 15(4):266–270. https://doi.org/10.1179/174329310X12726496072400
179. Gao M, Mei S, Wang Z, Li X, Zeng X (2012) Characterisation of laser welded dissimilar Ti/steel joint using Mg interlayer. Sci Technol Weld Joi 17(4):269–276
180. Davis J (1994) Aluminium and aluminium alloy. ASM Speciality Handbook. ASM International, USA
181. Majumdar B, Galun R, Weisheit A, Mordike B (1997) Formation of a crack-free joint between Ti alloy and Al alloy by using a high-power CO_2 laser. J Mater Sci 32(23):6191–6200. https://doi.org/10.1023/A:1018620723793
182. Vaidya W, Horstmann M, Ventzke V, Petrovski B, Koçak M, Kocik R, Tempus G (2010) Improving interfacial properties of a laser beam welded dissimilar joint of aluminium AA6056 and titanium Ti6Al4V for aeronautical applications. J Mater Sci 45(22):6242–6254. https://doi.org/10.1007/s10853-010-4719-6
183. Vaidya W, Horstmann M, Ventzke V, Petrovski B, Koçak M, Kocik R, Tempus G (2009) Structure-property investigations on a laser beam welded dissimilar joint of aluminium AA6056 and titanium Ti6Al4V for aeronautical applications. Part II: Resistance to fatigue crack propagation and fracture. Materialwiss Werkst 40(10):769–779. https://doi.org/10.1002/mawe.200900367
184. J-m N, L-q L, Y-b C, X-s F (2007) Characteristics of laser welding-brazing joint of Al/Ti dissimilar alloys. Chin J Nonferrous Metals 17(4):617
185. Lee S-JN, Hiroshi, Kawahito Y, Katayama S (2013) Weldability of Ti and Al dissimilar metals using single-mode fiber laser. J Laser Micro Nanoen 8(2):149–154. https://doi.org/10.2961/jlmn.2013.02.0006
186. Lee S-J, Takahashi M, Kawahito Y, Katayama S (2015) Microstructural evolution and characteristics of weld fusion zone in high speed dissimilar welding of Ti and Al. Int J Precis Eng Man 16(10):2121–2127. https://doi.org/10.1007/s12541-015-0274-z
187. Sahul M, Sahul M, Vyskoc M, Caplovic L, Pasak M (2017) Disk laser weld brazing of AW5083 aluminum alloy with titanium grade 2. J Mater Eng Perform 26(3):1346–1357. https://doi.org/10.1007/s11665-017-2529-6
188. Casalino G, Mortello M, Peyre P (2015) Yb–YAG laser offset welding of AA5754 and T40 butt joint. J Mater Process Technol 223:139–149. https://doi.org/10.1016/j.jmatprotec.2015.04.003
189. Kreimeyer M, Wagner F, Vollertsen F (2005) Laser processing of aluminum–titanium-tailored blanks. Opt Laser Eng 43(9):1021–1035. https://doi.org/10.1016/j.optlaseng.2004.07.005
190. Song Z, Nakata K, Wu A, Liao J (2013) Interfacial microstructure and mechanical property of Ti6Al4V/A6061 dissimilar joint by direct laser brazing without filler metal and groove. Mater Sci Eng A 560:111–120. https://doi.org/10.1016/j.msea.2012.09.044
191. Tomashchuk I, Sallamand P, Cicala E, Peyre P, Grevey D (2015) Direct keyhole laser welding of aluminum alloy AA5754 to titanium alloy Ti6Al4V. J Mater Process Technol 217:96–104. https://doi.org/10.1016/j.jmatprotec.2014.10.025
192. Chen S, Yang D, Li M, Zhang Y, Huang J, Yang J, Zhao X (2016) Laser penetration welding of an overlap titanium-on-aluminum configuration. Int J Adv Manuf Technol 87(9-12):3069–3079. https://doi.org/10.1007/s00170-016-8732-z
193. Chen SH, Li LQ, Chen YB, Liu DJ (2010) Si diffusion behavior during laser welding-brazing of Al alloy and Ti alloy with Al-12Si filler wire. Trans Nonferrous Metals Soc China 20(1):64–70. https://doi.org/10.1016/S1003-6326(09)60098-4
194. Chen S, Li L, Chen Y (2010) Interfacial reaction mode and its influence on tensile strength in laser joining Al alloy to Ti alloy. Mater Sci Tech-Lond 26(2):230–235. https://doi.org/10.1179/174328409X399056
195. Chen SH, Li LQ, Chen YB, Huang JH (2011) Joining mechanism of Ti/Al dissimilar alloys during laser welding-brazing process. J Alloy Compd 509(3):891–898. https://doi.org/10.1016/j.jallcom.2010.09.125
196. Peyre P, Berthe L, Dal M, Pouzet S, Sallamand P, Tomashchuk I (2014) Generation and characterization of T40/A5754 interfaces with lasers. J Mater Process Technol 214(9):1946–1953. https://doi.org/10.1016/j.jmatprotec.2014.04.019
197. Chen Y, Chen S, Li L (2009) Effects of heat input on microstructure and mechanical property of Al/Ti joints by rectangular spot laser welding-brazing method. Int J Adv Manuf Technol 44(3): 265–272. https://doi.org/10.1007/s00170-008-1837-2
198. Möller F, Grden M, Thomy C, Vollertsen F (2011) Combined laser beam welding and brazing process for aluminium titanium hybrid structures. Phys Procedia 12:215–223. https://doi.org/10.1016/j.phpro.2011.03.028
199. Chen S, Li L, Chen Y, Dai J, Huang J (2011) Improving interfacial reaction nonhomogeneity during laser welding–brazing aluminum to titanium. Mater Des 32(8-9):4408–4416
200. Caiazzo F, Alfieri V, Cardaropoli F, Sergi V (2013) Butt autogenous laser welding of AA 2024 aluminium alloy thin sheets with a Yb: YAG disk laser. Int J Adv Manuf Technol 67(9-12):2157–2169. https://doi.org/10.1007/s00170-012-4637-7
201. Gao M, Chen C, Gu YZ, Zeng XY (2014) Microstructure and tensile behavior of laser arc hybrid welded dissimilar Al and Ti alloys. Materials 7(3):1590–1602
202. Kulekci MK (2008) Magnesium and its alloys applications in automotive industry. Int J Adv Manuf Technol 39(9):851–865. https://doi.org/10.1007/s00170-007-1279-2
203. Gao M, Wang ZM, Li XY, Zeng XY (2012) Laser keyhole welding of dissimilar Ti-6Al-4V titanium alloy to AZ31B magnesium alloy. Metall Mater Trans A 43a(1):163–172. https://doi.org/10.1007/s11661-011-0825-6
204. Gao M, Wang Z, Yan J, Zeng X (2011) Dissimilar Ti/Mg alloy butt welding by fibre laser with Mg filler wire—preliminary study. Sci Technol Weld Join 16(6):488–496. https://doi.org/10.1179/1362171811Y.0000000033
205. Zhang Z, Tan C, Wang G, Chen B, Song X, Zhao H, Li L, Feng J Laser welding-brazing of immiscible AZ31B Mg and Ti-6Al-4V alloys using an electrodeposited Cu interlayer. J Mater Eng Perform 1-13
206. Liu J, Ventzke V, Staron P, Brokmeier HG, Oehring M, Kashaev N, Huber N (2012) Effect of dual-laser beam welding on

microstructure properties of thin-walled γ-TiAl based alloy Ti-45Al-5Nb-0.2C-0.2B (TNB). Tms 2012 141st Annual Meeting & Exhibition - Supplemental Proceedings, Vol 1: Materials Processing and Interfaces:887-894. https://doi.org/10.1002/9781118356074.ch111
207. Goldak JA, Akhlaghi M (2005) Computational welding mechanics. Springer Science & Business Media, New York
208. Rossini NS, Dassisti M, Benyounis KY, Olabi AG (2012) Methods of measuring residual stresses in components. Mater Des 35:572–588. https://doi.org/10.1016/j.matdes.2011.08.022
209. Taljat B, Radhakrishnan B, Zacharia T (1998) Numerical analysis of GTA welding process with emphasis on post-solidification phase transformation effects on residual stresses1. Mater Sci Eng A 246(1-2):45–54
210. Chuan L, Jianxun Z, Jing N (2009) Numerical and experimental analysis of residual stresses in full-penetration laser beam welding of Ti6Al4V alloy. Rare Metal Mat Eng 38(8):1317–1320
211. Cao XJ, Debaecker G, Jahazi M, Marya S, Cuddy J, Birur A (2010) Effect of post-weld heat treatment on Nd: YAG laser welded Ti-6Al-4V alloy quality. Thermec 2009(Pts 1-4 638-642):3655-+. https://doi.org/10.4028/www.scientific.net/MSF.638-642.3655
212. Wang G, Wu A, Zou G, Zhao Y, Chen Q, Ren J (2009) Bending properties and fracture behavior of Ti-23Al-17Nb alloy laser beam welding joints. Tsinghua Sci Technol 14(3):293–299. https://doi.org/10.1016/S1007-0214(09)70043-4
213. Wang GQ, Wu AP, Zhao Y, Zou GS, Chen Q, Ren JL (2010) Effect of post-weld heat treatment on microstructure and properties of Ti-23Al-17Nb alloy laser beam welding joints. Trans Nonferrous Metals Soc China 20(5):732–739. https://doi.org/10.1016/S1003-6326(09)60206-5
214. Short A (2009) Gas tungsten arc welding of α+ β titanium alloys: a review. Mater Sci Tech-Lond 25(3):309–324. https://doi.org/10.1179/174328408X389463
215. Lin GM (2017) Research on welding process of titanium alloy. DEStech Transactions on Engineering and Technology Research (mcee)
216. Petrov G, Khatuntsev A (1975) Chemical reactions role in pores formation during welding of titanium alloys. Svar Proizvod 57-58
217. Kabir A, Cao X, Medraj M, Wanjara P, Cuddy J, Birur A (2010) Effect of welding speed and defocusing distance on the quality of laser welded Ti–6Al–4V. In: Proceedings of the Materials Science and Technology (MS&T) 2010 Conference, Houston, TX, pp 2787-2797
218. EN B4678 (2011) Aerospace series. Weldments and brazements for aerospace structures joints of metallic materials by laser beam welding quality of weldments
219. Li Z, Gobbi S, Norris I, Zolotovsky S, Richter K (1997) Laser welding techniques for titanium alloy sheet. J Mater Process Technol 65(1-3):203–208. https://doi.org/10.1016/S0924-0136(96)02263-7
220. Chen HC, Pinkerton AJ, Li L (2011) Fibre laser welding of dissimilar alloys of Ti-6Al-4V and Inconel 718 for aerospace applications. Int J Adv Manuf Technol 52(9-12):977–987. https://doi.org/10.1007/s00170-010-2791-3
221. Fang X, Zhang J (2014) Effect of underfill defects on distortion and tensile properties of Ti-2Al-1.5 Mn welded joint by pulsed laser beam welding. Int J Adv Manuf Technol 74(5-8):699–705. https://doi.org/10.1007/s00170-014-6033-y
222. Karlsson J, Norman P, Kaplan AF, Rubin P, Lamas J, Yañez A (2011) Observation of the mechanisms causing two kinds of undercut during laser hybrid arc welding. Appl Surf Sci 257(17):7501–7506. https://doi.org/10.1016/j.apsusc.2011.03.068
223. Cerit M, Kokumer O, Genel K (2010) Stress concentration effects of undercut defect and reinforcement metal in butt welded joint. Eng Fail Anal 17(2):571–578. https://doi.org/10.1016/j.engfailanal.2009.10.010
224. Fabbro R (2010) Melt pool and keyhole behaviour analysis for deep penetration laser welding. J Phys D Appl Phys 43(44):445501. https://doi.org/10.1088/0022-3727/43/44/445501
225. Society AW (2001) Specification for fusion welding for aerospace application. AWS D17.1, Miami
226. Fang XY, Zhang JX (2016) Microstructural evolution and mechanical properties in laser beam welds of Ti-2Al-1.5Mn titanium alloy with transversal pre-extrusion load. Int J Adv Manuf Technol 85(1-4):337–343. https://doi.org/10.1007/s00170-015-7930-4